

GROWTH AND APPLICATIONS OF CARBON NANOTUBE-BASED NANOSPONGE
SHEETS

A THESIS SUBMITTED TO THE GRADUATE DIVISION OF THE UNIVERSITY OF
HAWAII AT MANOA IN PARTIAL FULFILLMENT OF THE REQUIREMENTS FOR THE
DEGREE OF

MASTER OF SCIENCE

IN

MECHANICAL ENGINEERING

December 2012

By

Benjamin Emmanuel Stein

Thesis Committee

Mehrdad N. Ghasemi Nejhad, Chairperson

Anthony Kuh

Scott Miller

We certify that we have read this thesis and that, in our opinion, it is satisfactory in scope and quality as a thesis for the degree of Master of Science in Mechanical Engineering.

THESIS COMMITTEE

Chairperson

ACKNOWLEDGMENTS

I would like to thank my advisor, Dr. Nejhad, for his guidance, patience, and support in my pursuit of my research. I would also like to thank my parents for keeping me honest and on track. It is a fact of life that you can never lie to your mother.

I would also like to thank the members of my research group for their assistance and for acting as sounding boards for my many crazy ideas: David Hummer for his help with the composites work, and Vamshi Gudapati for helping with the fuel cell experiments. Thanks to Tina M. Weatherby of the University of Hawaii Pacific Biosciences Research Center Biological Electron Microscope Facility for her help with the SEM and TEM imaging, and the sputter coating. Lastly, I would like to thank the fine state of Hawaii for providing the best research atmosphere a young scientist without any familial obligations could ask for.

ABSTRACT

Recently, while trying to replicate research results from Gui et al. [1], via liquid-injection chemical vapor deposition, an unexpected result was recorded-instead of growing a carbon nanotube sponge on the sample slide as expected, a thin, paper-like film was discovered on the furnace sidewalls. This material was found to have a flexibility and thickness comparable to Teflon tape, capable of being easily handled without tearing. Later SEM analysis showed that this new material was indeed comprised entirely of carbon nanotubes, but with a higher degree of long-range order, flexibility and toughness than the structures reported by Gui et al. indicating that this might be a new material type entirely, and hence is called NanoSponge Sheets (NSSs).

After repeating the conditions responsible for the initial discovery, it was determined that the major influencing factor was the addition of xylene to the precursor mix. Further experimentation yielded a functional set of growth parameters, which are still being further refined.

Currently, the growth process is being developed to grow larger sizes of the NSSs for further applications testing. The growth process is based on liquid-injection chemical vapor deposition, with a 2” diameter quartz furnace tube. A 6” diameter furnace is currently under development for use in other projects, but can be easily refitted for growing larger NSS samples for larger-scale applications and testing.

This “Nano Sponge Sheet” or NSS material has already displayed numerous interesting properties which may make it useful for a range of applications, including but not limited to: supercapacitors, energy storage, water desalination filters, composites/armor, EMF shielding, photovoltaics, and heat sinks.

TABLE OF CONTENTS

ABSTRACT	iv
Chapter 1	1
INTRODUCTION	1
1.1. Nanotechnology	1
1.2. Carbon Nanotube “Nanosponges”	3
1.3. Motivation	8
1.4. Goals.....	9
1.5. Organization of Thesis	10
Chapter 2.....	11
Manufacturing Methodology and Material System	11
2.1. Introduction	11
2.2. Prior Work: Carbon nanotube sponges	11
2.3. CVD Growth Process	13
2.4. Material System.....	14
2.4.1. Initial Structure	14
2.4.2. Growth Process Evolution	17
2.4.3. Improved Structure	19
Chapter 3	23
Growth Process	23

3.1.	Introduction	23
3.2.	Growth Parameters for Carbon Nanotube Nano-Sponge Sheets (NSSs).....	23
3.2.1.	Liquid Precursor Preparation	23
3.2.2.	Precursor Injection Rates	24
3.2.3.	Gas Mixes and Flow Rates	24
3.2.4.	Furnace and Evaporator Heating	24
3.3.	Growth Process for Carbon Nanotube NSSs.....	24
3.3.1.	Experimental Setup.....	24
3.3.2.	Precursor Injection Mechanism	25
3.3.3.	Gas Flow Controllers	26
3.3.4.	Evaporator Setup.....	27
3.3.5.	Exhaust Setup.....	28
3.3.6.	Sample Retrieval Process.....	28
Chapter 4	29
Processing Results, Characterization, and Discussion	29
4.1.	Processing Results for Manufactured NSSs.....	29
4.2.	Characterization Results of NSS	32
4.2.1.	Scanning Electron Microscopy (SEM)	32
4.2.2.	Transmission Electron Microscopy (TEM)	35
4.2.3.	Raman Spectroscopy.....	39

4.3. Discussion	41
Chapter 5	43
Performance Evaluations, Densification, and Functionalization	43
5.1. Introduction	43
5.2. Cleaning Tests	43
5.2.1. Sonication in Ethanol	44
5.2.2. Flame Test	46
5.3. Densification	49
5.4. Acid Treatment Functionalization	51
Chapter 6	54
Preliminary Applications	54
6.1. Introduction	54
6.2. Fuel Cell Applications of NSSs	54
6.2.1. Sputter Coating	56
6.3. Composites	58
Chapter 7	62
Potential Applications	62
7.1. Introduction	62
7.2. Structural	63
7.3. Non-Structural	64

Chapter 8	67
Conclusions and Future Work	67
REFERENCES	69

LIST OF FIGURES

Figure 1 A Multi-Walled Carbon Nanotube.	2
Figure 2 As-grown CNT sponge sample [33].	4
Figure 3 Demonstrating the flexibility of a sponge sample [20].	5
Figure 4 SEM micrograph showing the sponge infrastructure [20].	5
Figure 5 Diagram showing the disordered sponge infrastructure [20].	6
Figure 6 Demonstration of the sponge's oil absorption abilities [19].	6
Figure 7 Demonstrating the mechanical flexibility and boron-induced elbows of the CNT sponge [23].	7
Figure 8 Demonstrating the oil absorption capacity of the sponge material [23].	8
Figure 9 Chemical Vapor Deposition via Liquid Injection [33].	12
Figure 10 CNT Sponge density and porosity vs source injection rate [20].	12
Figure 11 The setup used for growth of nanotube sponges by Gui et al. [picture provided by authors upon request]	13
Figure 12 Initial NSS discovery sample.	15
Figure 13 SEM image showing creases in the NSS surface.	16
Figure 14 NSS surface showing directionality of nanotube infrastructure.	17
Figure 15 Approximate thickness of initial NSS sample is 20 microns.	17
Figure 16: One example of an experimental substrate.	19
Figure 17 Current NSS sample, with detail of surface “bumps”.	20
Figure 18 Larger view of the new NSS material, showing the increase in sample thickness.	21
Figure 19 Close-up view of new NSS material, showing aligned bundles of CNTs, with a disordered underlayer.	21

Figure 20 Surface view of NSS material, showing similar long-range order of CNTs.	22
Figure 21 CVD furnace and assembled components in the Hawaii Nanotechnology Laboratory. (Note that furnace is pushed in to minimize distance between injected precursor and furnace, minimizing condensation).....	25
Figure 22 Disposable injection syringe mounted on injection pump, with Swagelok adapter and tubing.	26
Figure 23 Mass Flow Controllers.	26
Figure 24 Evaporator assembly with steel chamber wrapped with heating tape, a fiberglass thermal insulator, and aluminum foil for insulation/overwrap.	27
Figure 25 Evaporator Power Supply and Temperature Control.	28
Figure 26 A unique and unexpected growth of “iron” crystals.	33
Figure 27 Transition between sponge "bulk" NSS and sponge "paper" NSS phases, indicating growth process may be nonlinear.	33
Figure 28 SEM image showing cross-linking between nanotubes, as well as kinks, bends, and other unique features.	34
Figure 29 Close-up image of an open nanotube end, with a scale bar showing the approximate diameter at 40nm, indicating that the nanotube is multi-walled.	35
Figure 30 Carbon nanotube partially filled with iron.	36
Figure 31: Carbon coated nanotube. Inner diameter is measured at 15 nm, the outer diameter at 26 nm, and the coating at 37 nm, indicating a 5.5 nm thick coating (TEM).	37
Figure 32 Carbon nanotube with irregular carbon coating (TEM).	38
Figure 33 Nanotubes showing irregular coatings and embedded iron cores (TEM).	39

Figure 34 Raman Spectrograph of NSS sample showing peaks around 1300, 1600, and 2600 cm^{-1}	40
Figure 35 NSS sample after sonication in ethanol for 5 minutes, where the SEM imaging shows removal of contaminants	44
Figure 36 Further imaging of sonicated NSS material, showing total deterioration of the ordered NSS infrastructure (SEM)	45
Figure 37 Higher magnification image of ethanol sonicated NSS sample (for 5 minutes), showing no damage to individual nanotubes (SEM)	46
Figure 38 NSS sample undergoing "flame test".	47
Figure 39 NSS sample shriveling near the end of the flame test, as trapped acetone is burned away.	47
Figure 40 NSS sample resumes its original shape immediately after the flame test, and can be handled without discomfort in terms of heat and temperature.	48
Figure 41 SEM image of NSS sample after flame test, showing unique iron catalyst crystal formations.	48
Figure 42 a) SEM images of the NSS surface after flame test (at the edges). b) showing fused clusters of metallic catalyst, with apparently undamaged nanotube infrastructure left intact.	49
Figure 43 SEM images of densified NSS samples, showing compressed layers of nanotubes, and reduced pore sizes. (large features, such as creases and curves, are still preserved).	50
Figure 44 SEM images of densified NSS showing surface impressions left by forcep tweezer grips, and a measured sample thickness of approximately 35 microns.	51
Figure 45 Tunable functionalization on hydrophobicity/hydrophilicity of the NSSs employing acid treatment.	52

Figure 46 Acid-treated NSS samples showing rougher nanotubes.....	53
Figure 47 Peak Power Density vs Relative Humidity. NSS GDLs perform better than standard carbon papers, but less than carbon paper enhanced by MWCNTs-based nanoforests.....	56
Figure 48 Sputter coating a gold/palladium layer on a NSS sample.	57
Figure 49 NSS surface sputter coated with Au/Pd.....	57
Figure 50 Higher magnification images of deposited Au/Pd island sputter coated on the NSS surface. Individual metal islands are approximately 10-20 nm in diameter.	58
Figure 51 Top and bottom of composite sample, showing cured pool of resin, with shiny surface and rougher underside.....	59
Figure 52 SEM images of composite surface, showing pools of resin (black), with distributed graphene platelets (gray) and underlying nanotube network (continuous lines).	60
Figure 53 TEM image showing nanotube partially filled with iron.	61

Chapter 1

INTRODUCTION

1.1. Nanotechnology

Nanotechnology is an emerging trend of multidisciplinary research focused on the development and study of atomic or molecular scale phenomena and technologies. In recent years, nanotechnology has become an exciting and intensely funded field of science, with nearly every major scientific entity contributing to research in some manner [2]. The field of nanotechnology applies to and has implications in nearly every field of study, from materials science to biotechnology. Numerous companies have sprung up to commercialize upon scientific breakthroughs, and most major corporations with research and development branches have devoted vast resources to building nanotechnology portfolios [3]. Still, since nanotechnology is such a new field, there is a great deal of work to be done before mature contributions will be made to the commercial space. This delay between research funding and sellable products has caused some short-sighted investors to label nanotechnology as another “bubble”, or as a passing fad [4]. Other groups, fearful of the unknown health and safety implications of nanomaterials and nanoparticulates, have called for severely restricting limitations to be placed on all nanotechnology research [5]. The contributions from nanotechnology are indeed meager and seemingly superficial for now, but as the field grows they will become more prevalent and more fundamentally enabling, like all new technologies.

Carbon nanotubes (See Figure 1), discovered in 1991 by Ijima et al. [6], have been one of the most intense areas of research in the field of nanomaterials, due to their many fascinating and promising qualities, including mechanical strength, conductivity, and chemical stability [7].

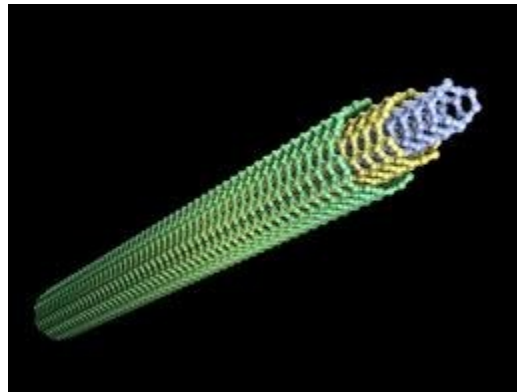


Figure 1. A Multi-Walled Carbon Nanotube.

Currently, there are a number of companies seeking to grow them commercially, and even more seeking to utilize them for other commercial uses, in everything from composite additives to combustible fuel enhancements [8]. Even more potential applications are being developed in research laboratories and universities, such as artificial muscles [9–11], bio sensors [12–14] and the next generation of transistors [15–18], to name a few.

A major limiting factor for nanotubes as a commercial material is their size and the limits of standard growth processes, which can grow pristine forests of nanotubes for use in research, or as additives in other process, but which are limited to small sizes; making it very difficult in transferring their nanoscale properties to macroscale applications. Countless papers have been published describing methods for growing longer nanotubes, some even continuously, but none have been able to demonstrate a material with properties even close to the theoretical limits of individual nanotubes. To date the longest nanotubes can be grown only a few centimeters [19],

and although films [20, 21], yarns [22–24] and aerogels [25–32] can be produced in labs, these are still agglomerations of individual nanotubes, and not continuous structures.

While these are interesting approaches and worthy of further research, they are still of the “top-down” approach, where the material strength relies upon the Van der Waals interactions between the nanotubes, and not on the nanotubes themselves. Even if further research improves the utility of such methods, it must be remembered that the more complicated a process is, the more difficult and expensive it will be to scale up for commercial applications.

Nanotechnology and the products developed from its research have the capability to radically simplify and transform the human condition and vastly expand our capabilities. This is a very exciting field with enormous potential, and we must remember that the success of one research group does not in any way limit the success of others- it simply shows that success is indeed possible and should serve as further motivation and guidance for others to follow.

1.2. Carbon Nanotube “Nanosponges”

Although much research has been conducted on carbon nanotubes, and macroscale structures containing nanotubes, the first work to show a structure of free-standing interconnected nanotubes, called a “sponge” was reported by Gui et al. in 2011 [1]. This paper was the initial focus of this research and could therefore be considered the “inspiration” for this work.

To grow their “nanosponges” Gui et al. injected a liquid precursor solution of ferrocene dissolved in dichlorobenzene into a quartz tube furnace, under a gas flow of hydrogen and argon. This process, commonly known as chemical vapor deposition (CVD), is very common and often the preferred method for the growth and study of carbon nanotubes. After a pre-determined amount of time, a sample slide was removed from the growth zone in the furnace, and the sponge sample was retrieved (see Figure 2).

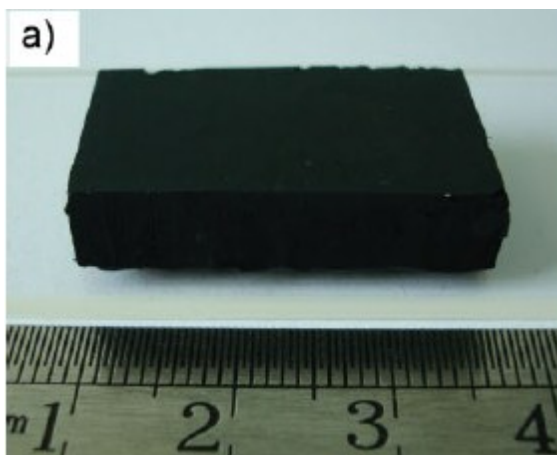


Figure 2. As-grown CNT sponge sample [33].

The sponge samples were shown to have a high degree of flexibility and mechanical integrity, and could even be twisted and handled without breaking (see Figure 3). Further SEM characterization revealed the high degree of disorder in the CNT infrastructure (see Figure 4), leading to the material's high porosity and low density (see Figure 5). This large surface area was found to be highly effective at absorbing large amounts of oil, giving credence to the “sponge” moniker (see Figure 6). Sponge density could be controlled by varying the injection rate of the precursor, while the thickness of the sponge was controlled by varying the growth time. Further studies showed the connections between the nanotubes were Van der Waals forces, and not covalent bonds or branched nanotubes.

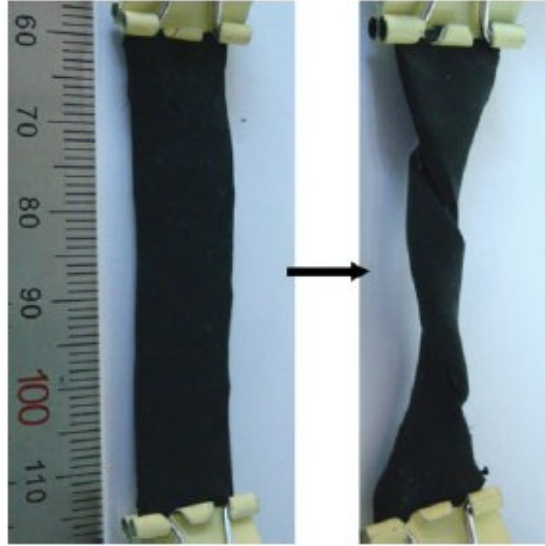


Figure 3. Demonstrating the flexibility of a sponge sample [33].

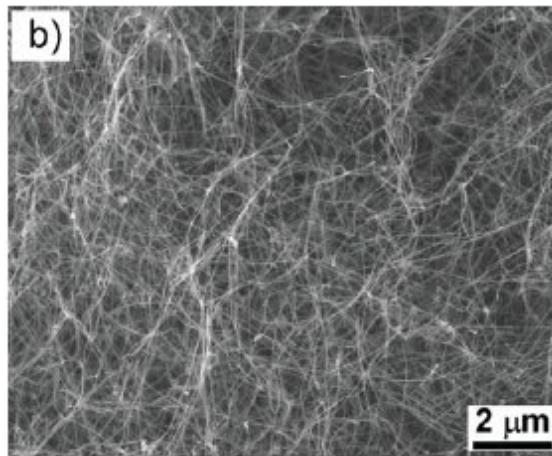


Figure 4. SEM micrograph showing the sponge infrastructure [33].

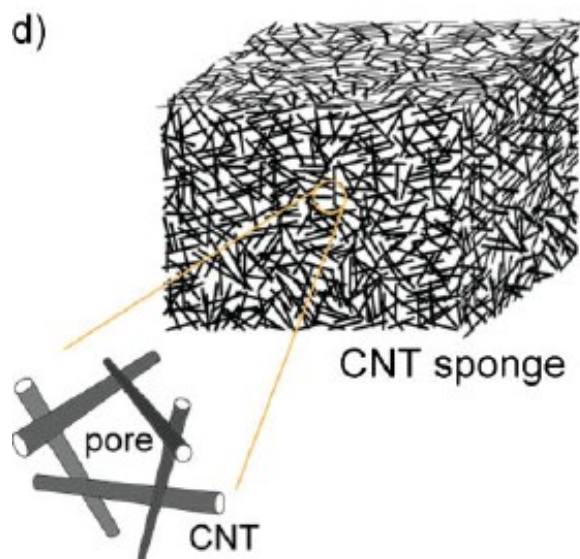


Figure 5. Diagram showing the disordered sponge infrastructure [33].

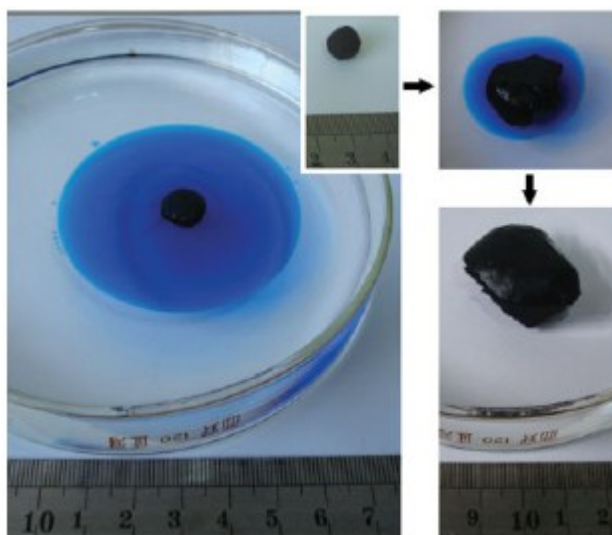


Figure 6. Demonstration of the sponge's oil absorption abilities [1].

More recently, Ajayan et al. from Rice University published a paper showing a similar process in which a sponge-like material is grown via chemical vapor deposition, demonstrating similar properties such as high porosity, low density, and mechanical flexibility [34]. The primary difference is in the chemistry of the injected liquid, which contains boron. It is reported that the

boron is responsible for inducing the distinctive “elbow” junctions seen in SEM micrographs, as well as covalent bonds between the nanotubes (see Figure 7). Similar to the sponge reported by Gui et al. [33] the boron sponge can be used repeatedly for oil absorption (see Figure 8). This is an exciting development, and may prove fruitful for future research avenues or collaborations.

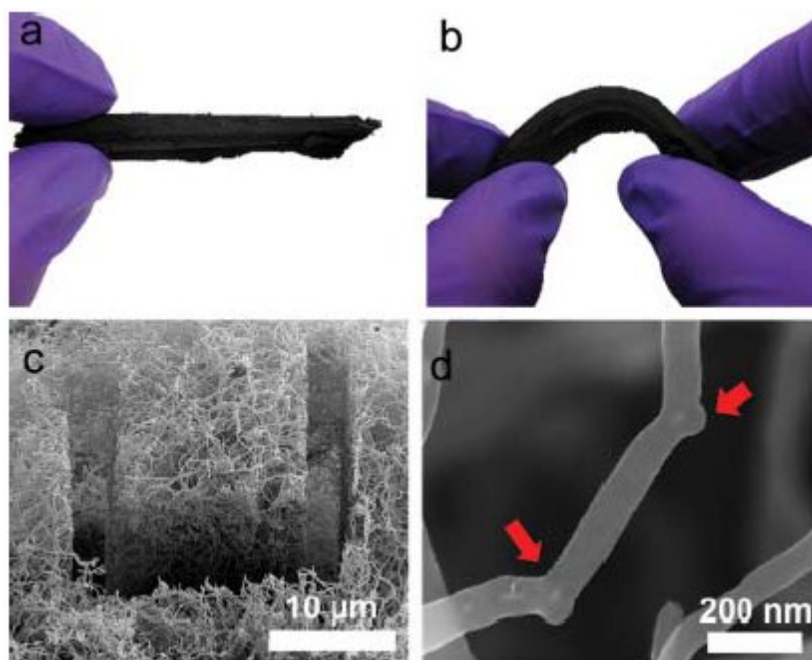


Figure 7. Demonstrating the mechanical flexibility and boron-induced elbows of the CNT sponge [34].

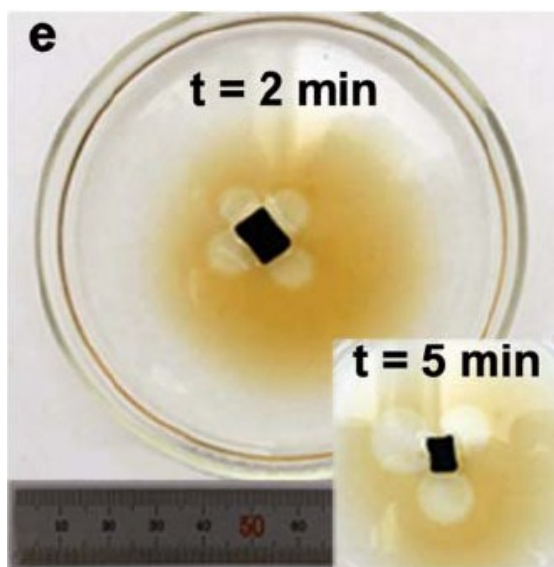


Figure 8. Demonstrating the oil absorption capacity of the sponge material [34].

1.3. Motivation

The main motivation behind this line of research is the creation of a material with nanoscale size and structures with micro- and macro-scale sizes, capable of being utilized as a normal material, but with nanoscale properties and features. For many years the materials science community has been pursuing this trend, attempting a top-down approach of reducing material feature sizes [35]. On the other hand, a “bottom-up” approach allows greater control over existing materials, and can even lead to new capabilities. Therefore, the “top-down” approach has begun to be replaced by a “bottom-up” approach in recent years, with the emergence of nanotechnology, and the notion of creating new structures by assembling their individual basic building blocks, i.e., atoms. This new methodology has allowed for far greater control over materials properties, and more efficient use of resources, as well as the discovery of new and interesting properties altogether [36].

Many applications, such as photovoltaics, energy storage, water filtration, and composites, have benefitted from the advent of new nanomaterials, and continue to be at the forefront of its

research. A few current companies actually advertise products incorporating nanomaterials, and have had varying degrees of commercial success [37].

Therefore, the main driving motivation behind this research, regardless of the actual methods used, was to develop a simple, scalable and reproducible method for creating macroscale structures comprised entirely of carbon nanotubes, in situ, with as little post processing as possible, and yet still displaying properties comparable to individual nanotubes. This is the main reason nanosponges were chosen as a starting point over films, aerogels, or yarns.

1.4. Goals

The initial goal of this research was to reproduce and then improve upon the carbon nanotube sponge work first developed by Gui et al. [33]. This, however, proved to be more problematic than expected, and a great deal of time and frustration was spent attempting to replicate the exact growth conditions described in the paper, and communicating with the authors to ask for help and clarification. Even then, the results described by Gui et al. [33] was not successfully reproduced. This was primarily due to a few experimental details which, although taken for granted by the authors and not included in their reports, were nonetheless vital for the growth process. Therefore, a great deal of work in this research has been invested in the preliminary process conditions for the development of “nanosponges”, when numerous interesting structures not described by Gui et al. [33] were found in this research, some of which could lead to other interesting avenues of research, explained in this thesis.

The deeper, underlying goal behind pursuing nanosponges in general is their uses as macroscale materials with nanoscale properties. Such structures have long been pursued as promising candidates for the next generation of energy storage technologies and structural composites [38–41]. There are countless other applications for nanomaterials, many of which will not even be

realized until the supporting technologies are mature enough to support them, leaving them for now as miracles inventions looking for a use.

Once the NSS material was discovered, the goal of this research effort shifted from attempting to reproduce nanosponges to pursuing this new line of research, with a focus on further understanding of the structural, thermal, and electrical properties of the NSS infrastructure. It was also clear that this research was outside the scope of a single Master's thesis, and so a second goal of the work was to lay the groundwork for a further PhD study of the material, with a clear path towards the development of a novel fuel cell components or energy storage device.

1.5. Organization of Thesis

This first chapter covers a basic overview of the field of nanotechnology and nanomaterials, particularly on carbon nanotubes, as well as the work done on nanosponges. Chapter 2 covers the methods utilized in the growth process and a basic overview of the Chemical Vapor Deposition process as well. Chapter 3 is concerned with specifics of growing the NSS materials, including equipment used and experimental parameters. Chapter 4 is concerned with the characterization techniques used to initially study the material and other characterization tests. Chapter 5 describes the properties and data produced by the characterization effort, and lessons learned by trial and error in the experimental section. Chapter 6 covers initial efforts at functionalization of the NSS material, and the results. Chapter 7 covers the potential future applications of the material, taking advantage of its material properties as well as its other electrical or thermal characteristics. Chapter 8 concludes and summarizes the thesis, and suggests avenues for future work and exploration, which will hopefully be pursued as part of a doctoral thesis.

Chapter 2

Manufacturing Methodology and Material System

2.1. Introduction

This chapter provides an overview of the process used by Gui et al. [1, 33] to grow their CNT sponge samples, including the effects of variations in the growth parameters. It also presents a brief overview of the Chemical Vapor Deposition (CVD) process, which is the method used to grow the sponges, and Nano-Sponge Sheets (NSSs).

The new NSS material will then be discussed, including the original discovery material, the parameters that were experimented with in developing the current growth protocol, and finally a description of the most current NSS developments.

2.2. Prior Work: Carbon nanotube sponges

The process used by Gui et al. [1, 33] for growing the carbon nanotube sponges utilized liquid injection chemical vapor deposition in a horizontal quartz tube furnace (see Figure 9).

A liquid precursor solution of ferrocene powder dissolved in 1,2-dichlorobenzene was prepared in proportions of .06g/mL, then injected into the hot furnace zone by a syringe pump at rates varying between 0.1-0.25 mL/min. Typical growth times for a sponge of 8mm thickness were 4 hours at a reaction temperature of 860°C. Argon, an inert carrier gas, was flowed at 2000 sccm, while hydrogen, used to prevent amorphous carbon buildup as well as to reduce the ferrocene into iron particles, was injected at 300 sccm. The sample substrate was a cleaned quartz glass

plate. It is reported that increasing the liquid injection rate increases both the sponge growth rate as well the sponge density (see Figure 10).

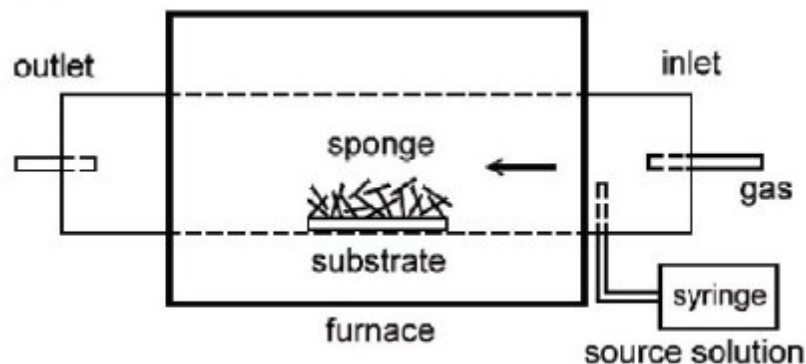


Figure 9. Chemical Vapor Deposition via Liquid Injection [33].

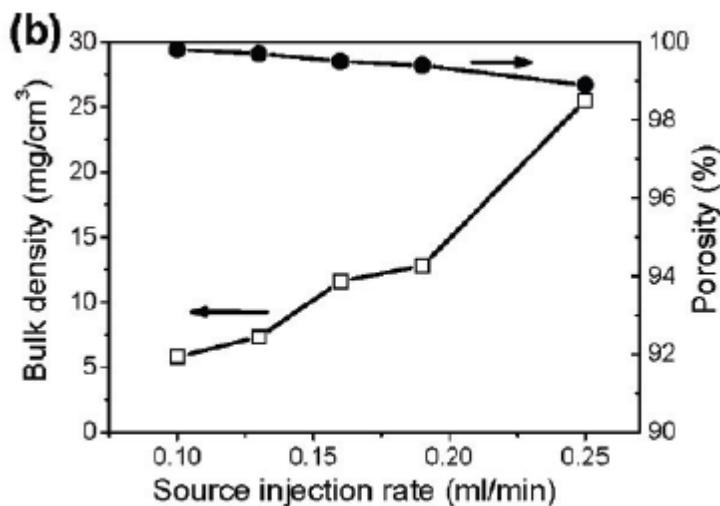


Figure 10. CNT Sponge density and porosity vs source injection rate [33].

A photograph of the actual setup, emailed at the author's request, is included in Figure 11. It is worth noting that there is no mention of the length of furnace tube exposed on either side of the furnace walls, nor of the actual injection nozzle, if any, used to inject the liquid precursor. In addition, there is no mention of the mechanism used to evaporate the liquid precursor (it is

assumed that the heating tape wrapped around the exposed furnace walls performs this function, though the temperature of heat tape remains a mystery). The importance of these seemingly minor details is not to be overlooked, as will be discussed in more detail in later sections.



Figure 11. The setup used for growth of nanotube sponges by Gui et al. [33]

2.3. CVD Growth Process

Chemical Vapor Deposition, or CVD, is a fairly common process typically used by the semiconductor industry for growing or depositing thin layers of material for use in integrated circuits. There are numerous variations of the CVD processes, and these are typically differentiated by operating pressure and temperature, physical characteristics of the vapor, plasma enhancements, and others with more unique and specialized features [42]. In a typical process, a substrate is exposed to one or several volatile vapor-phase precursors, which decompose or react with the substrate surface to produce the desired solid deposit. This is typically the result of chemical reactions which can produce noxious byproducts, and must be

removed with a persistent gas flow. In typical CVD systems designed to grow carbon nanotubes, a carbon feedstock such as methane, acetylene, or xylene is combined with a metallic catalyst, typically ferrocene, under an inert atmosphere of argon and hydrogen. In more sophisticated systems where nanotube purity and alignment are desired, plasma enhancement is typically utilized, which lowers the required reaction temperatures and reduces waste products.

Currently, the CVD system is the most commonly used choice for researchers growing carbon nanotubes due to its low cost, ease of operation, and flexibility.

Other methods commonly used to grow carbon nanotubes include: arc discharge, laser ablation, high-pressure carbon monoxide (HiPCo) and natural pyrolysis (fire).

2.4. Material System

2.4.1. Initial Structure

The initial discovery of the nano-sponge sheet material was found after a failed attempt to grow a nano-sponge using the protocols described by Gui et al. After a 4 hour test run, no sponge samples were recovered from the sample slides. However, a few sections of paper-thin material were scraped off of the sidewalls of the furnace tube (see Figure 12).



Figure 12. Initial NSS discovery sample.

The samples were as thin as paper, and could be easily folded and flexed without tearing or crumbling, with a surface texture almost similar to Teflon tape. Interestingly, the samples could be folded upon themselves many times, and still returned to their normal shapes without any evidence of creases or deformation. Considering the growth time and thickness, it was determined that these samples were altogether novel and different from anything reported by Gui et al. Scanning Electron Microscopy revealed further details indicating the novelty of this new material—firstly that the surface already had numerous folds and deformations, but whether caused by bulk stresses or natural processes is impossible to know at this time (see Figure 13).

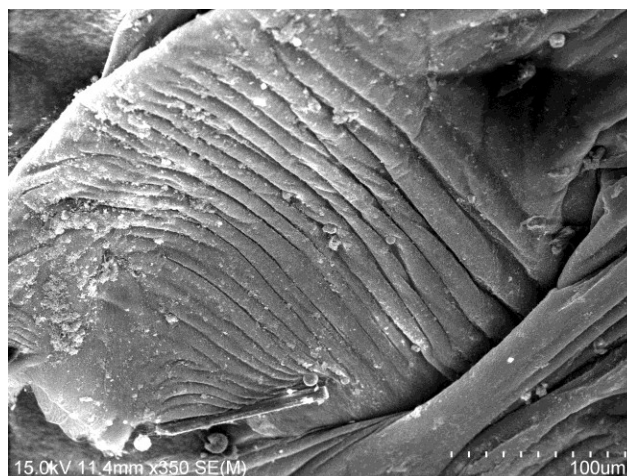


Figure 13. SEM image showing creases in the NSS surface.

Further analysis of the NSS surface morphology showed an interesting long-range alignment of the carbon nanotube infrastructure, most likely oriented in the direction of gas flow. Although short-range disorder was present, similar to the images reported for nanosponges, surface layers displayed a degree of cross-linking and directionality not seen anywhere else (see Figure 14). Attempts to accurately measure the thickness of the sample proved fruitless both due to its conformability and its extreme thinness. Still, a sample was placed on its side in an SEM chamber and an edge was measured, showing an approximate thickness of 20 microns (see Figure 15). Considering that they are composed entirely of as-grown carbon nanotubes, these initial NSS samples indicate one of the most promising examples thus far of creating a macroscale material with nanoscale properties.

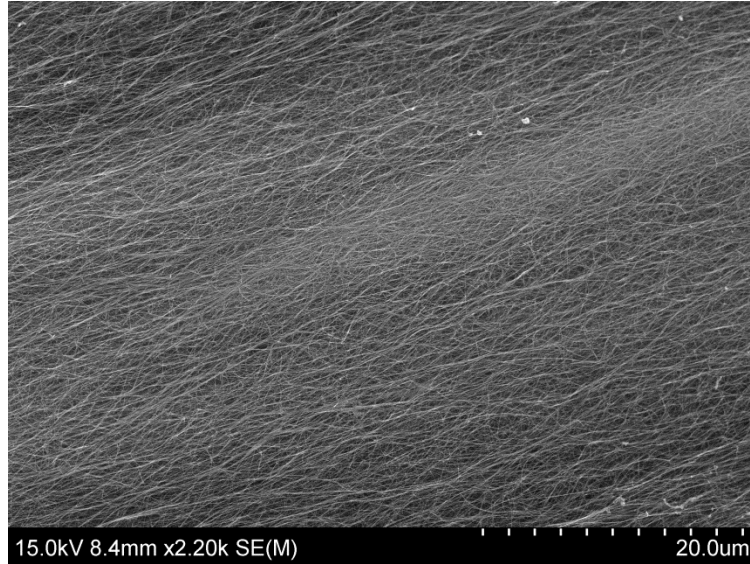


Figure 14. NSS surface showing directionality of nanotube infrastructure.

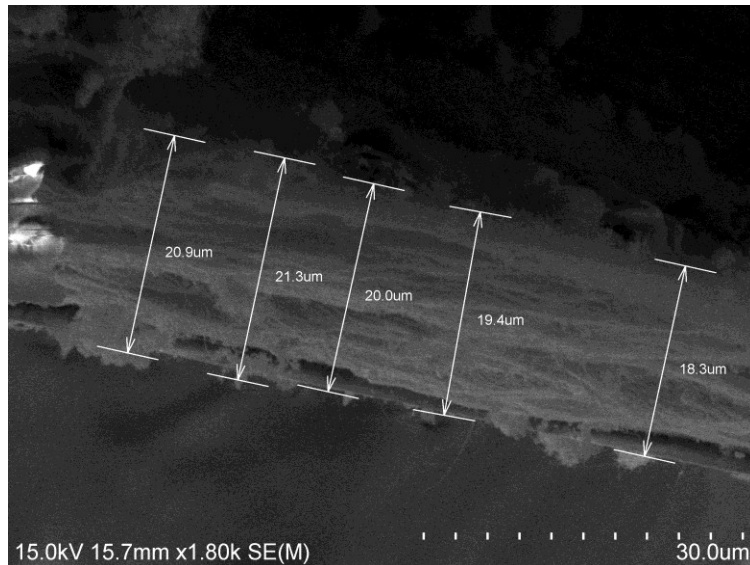


Figure 15. Approximate thickness of initial NSS sample is 20 microns.

2.4.2. Growth Process Evolution

Several experimental parameters underwent systematic variations in order to determine the optimal set of experimental conditions. It is important to note that this is an ongoing process, and as such a number of different parameters have remained unchanged, while the importance of

other factors remain unknown and to be determined in future studies. It should also be taken into account that due to the relative novelty of this process, all tests were qualitative in nature, with a simple visual examination of the sample slides and sidewalls of the furnace tube determining the relative impact of the change in experimental conditions. In future work more effort will be devoted to modeling the growth process in an attempt to predict and optimize the experimental parameters and thereby obtain consistent sample sizes, allowing for more consistent and quantitative verification of test results.

The experimental variables include:

- The furnace temperature
- The evaporation chamber temperature
- The flow rates of both the argon and hydrogen lines
- The position of the injection side of the furnace tube relative to the furnace
- The type of inlet (single or double)
- The ratio of xylene and dichlorobenzene
- The injection rate of the precursor
- The material type, shape, and position of the sample substrate

Another important factor is sample retrieval. After the NSS material has been deposited successfully on a quartz sample slide, it must be removed with a razor blade, which can cause mechanical damage and may not always remove all the material. Alternatives include chemical treatments such as etchants to remove the top silicon dioxide layer of the quartz sample slide, but these etchants are often very dangerous to handle, so will be used as a last resort if no safer alternatives can be found. Since this process is being developed with commercial applications in

mind, several iterations of substrate materials and shapes were developed in an attempt to maximize the amount of NSS material retrieved per test run. Figure 16 shows a custom-ordered quartz tube shell insert, designed to be removed from the furnace tube for maximum material yield. The different growth regions and gas flow are clearly visible in the figure. The gray zone is amorphous soot, while the black zone is the NSS region. The extra quartz tube added another thermal layer, and hence changed the gas flow dynamics, leading to unexpected results. While a 1"x 3" sample slide might be acceptable for developing the process for research purposes, any attempts to increase production output or deposition area will require a dramatic rethinking of the entire horizontal tube furnace design. This is one of the major hurdles for the entire fledgling nanotube industry, and is not a task to be taken lightly.



Figure 16. One example of an experimental substrate.

2.4.3. Improved Structure

A functional set of experimental parameters has been developed via trial and error, yielding more uniform NSS samples over a larger sample area (see Figure 17). These new samples demonstrate the same flexibility and durability as the initial NSS samples, but can be grown over a larger area, and with controllable thickness (see Figure 18). In addition, the growth zone inside the furnace tube is larger, allowing more material to be retrieved per test run and more post-

processing experiments to be performed. Most importantly, the process is now reproducible, changing the status of the NSS material from an accidental discovery to a working laboratory prototype. As the SEM images show, the new NSS material has similar long-range order as the initial discovery material, but is obviously not a perfect production yet, having fewer CNT bundles and more catalyst particles on the surface (see Figure 19 and Figure 20).

Another puzzling issue with the current process is the presence of “bumps”, or isolated circular/hemispherical growths distributed across the surface of the sample (see Figure 17). These are actually similar to the clustered growths seen while attempting to reproduce the original CNT sponge structure. These features indicate that the current process still needs further improvements. Certainly, more investigations are required and, in time, these features may prove to be another discovery in their own right.

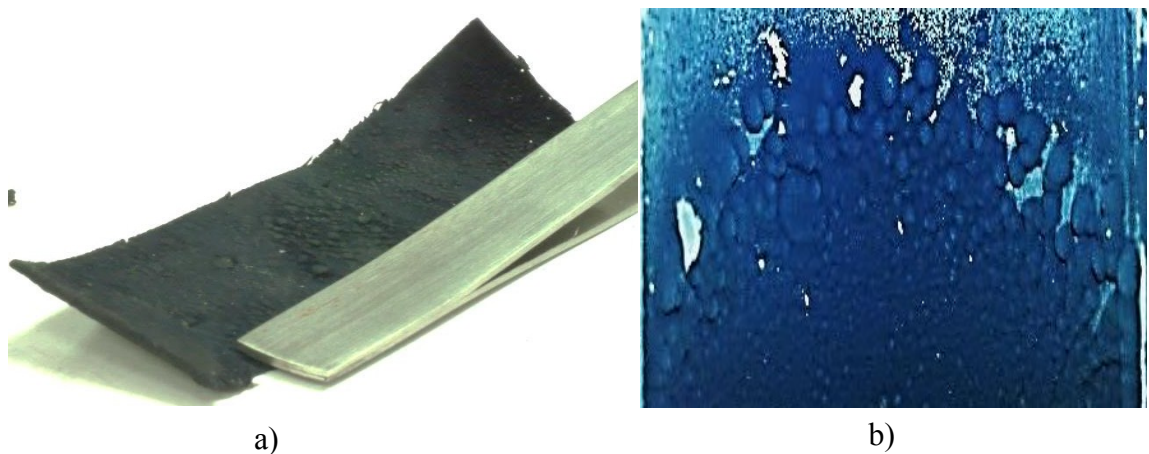


Figure 17. a) Current NSS sample, b) detail of surface “bumps”.

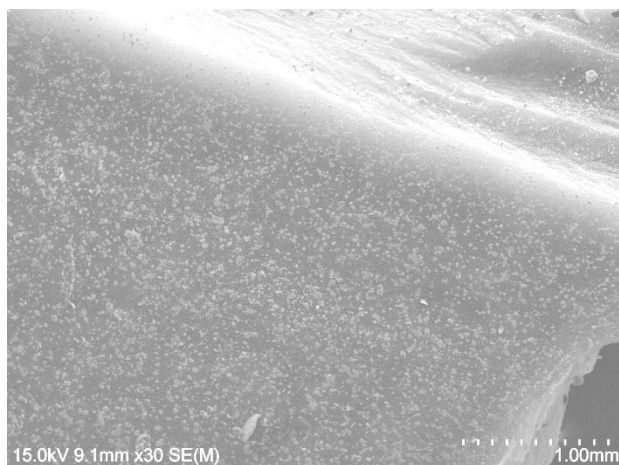


Figure 18. Larger view of the new NSS material, showing the increase in sample thickness.

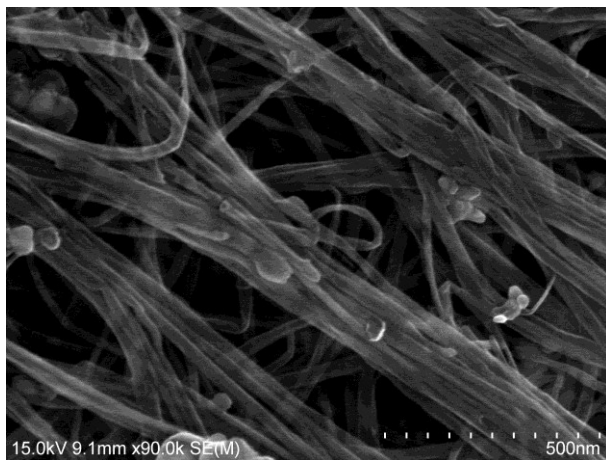


Figure 19. Close-up view of new NSS material, showing aligned bundles of CNTs, with a disordered underlayer.

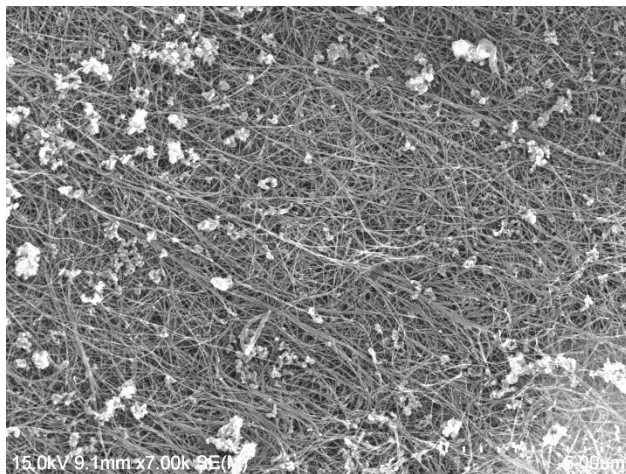


Figure 20. Surface view of NSS material, showing similar long-range order of CNTs.

Chapter 3

Growth Process

3.1. Introduction

A working set of experimental parameters has been established for producing repeatable test results. Note that these parameters are only for the most current working process. Since there was no theoretical or computational modeling done prior to this work, all of these parameters were developed purely through trial and error in an experimental setting. Given the purely qualitative nature of this study, it can be assumed that with further characterization and experimentation, these parameters are likely to improve. It is also likely that several variations of the NSS material will be developed, and different sets of experimental parameters will need to be established.

3.2. Growth Parameters for Carbon Nanotube Nano-Sponge Sheets (NSSs)

3.2.1. Liquid Precursor Preparation

The liquid precursor contained the carbon feedstock and iron catalyst. Xylene [43] and 1,2-dichlorobenzene [44] were combined in a 1:3 ratio, then ferrocene [45] was added and the solution was sonicated approximately 3 minutes or until fully dissolved. For a 20 mL solution, the standard amount used with the following proportions:

- 5 ml Xylene
- 15 ml 1,2-dichlorobenzene
- 0.9 g ferrocene

3.2.2. Precursor Injection Rates

Liquid precursor was injected at a rate controlled via the syringe injection pump computer control mechanism, which calculated the motor speed based upon the user-input syringe inner diameter. For standard NSS growth runs, the precursor injection rate was kept at 0.15 ml/min.

3.2.3. Gas Mixes and Flow Rates

Gas flow rates were controlled via a pair of mass flow controllers. The Argon flow was set at 1500 sccm, and the Hydrogen flow rate was set at 300 sccm.

3.2.4. Furnace and Evaporator Heating

The furnace temperature was set via computer control, and kept constant at 830°C. The heating tape wrapped around the evaporator tube was held at approximately 186°C.

3.3. Growth Process for Carbon Nanotube NSSs

3.3.1. Experimental Setup

The fully assembled experimental setup, seen in Figure 21, is an existing CVD system in the Hawaii Nanotechnology Lab and is very similar to the setup described by Gui et al. [33] with a few notable exceptions. Firstly, the gasses are mixed with liquid precursor in the evaporation chamber, then evaporated and injected into the furnace tube as close to the furnace heat zone as possible. There is no heating tape, there is only a single injection nozzle, and the overall volume of the furnace tube is noticeably smaller.



Figure 21. CVD furnace and assembled components in the Hawaii Nanotechnology Laboratory. (Note that furnace is pushed in to minimize distance between injected precursor and furnace, minimizing condensation).

The furnace used was a Thermolyne 79300 equipped with a digital temperature controller. The furnace is designed for a furnace tube of 2" diameter, and has a maximum temperature of 1200°C.

3.3.2. Precursor Injection Mechanism

The injection pump used was a NE-1000, from New Era Pump Systems, Inc with programmable inputs, step-motor control, and a minimum pumping rate of 0.73 $\mu\text{L/hr}$.

The syringes used were designed for single use, featuring a Luer-lock tip with an inner diameter of 28mm and a maximum capacity of 60mL. They were purchased in bulk from McMaster-Carr. Figure 22 shows the detailed assembly of the syringe mount.



Figure 22. Disposable injection syringe mounted on injection pump, with Swagelok adapter and tubing.

3.3.3. Gas Flow Controllers

Gas flows were regulated by a pair of mass flow controllers (MFCs) manufactured by Alicat Scientific, of the MCS series (see Figure 23). Both MFCs are rated to be accurate to $\pm 2\%$. The argon MFC had a maximum rated flow rate of 5 SLPM, and the hydrogen MFC had a maximum flow rate of 1 SLPM. All gas lines were Teflon-lined Tyvex polymer, with standard $\frac{1}{4}$ " Swagelok gas fittings.



Figure 23. Mass Flow Controllers.

3.3.4. Evaporator Setup

The liquid precursor was evaporated in a steel vessel prior to injection into the growth zone (see Figure 24). It is important to note here that the mechanism used to control the temperature of the evaporation vessel was changed during the course of the research effort, to allow for greater control. Initially, the power for the heating tape came from a Variac variable voltage regulator, with a thermocouple readout showing the approximate temperature of the vessel. The voltage and temperature had to be carefully monitored to maintain optimal conditions, which could often complicate the growth process. Therefore, a PID temperature controller was obtained from Oven Industries, Inc which automatically regulated the heating tape voltage to match the desired temperature via thermocouple feedback loop (see Figure 25). This has allowed for relatively trouble-free operation.

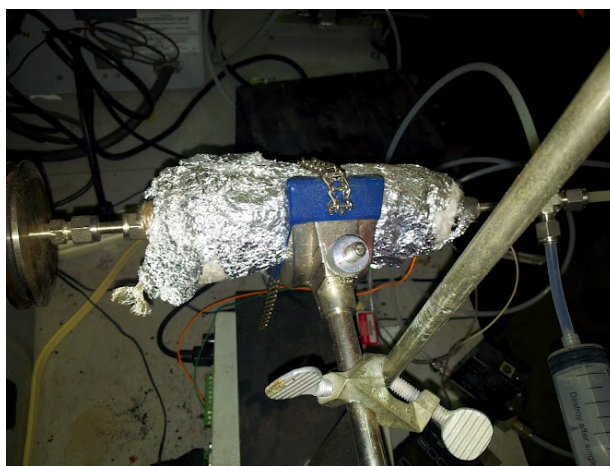


Figure 24. Evaporator assembly with steel chamber wrapped with heating tape, a fiberglass thermal insulator, and aluminum foil for insulation/overwrap.

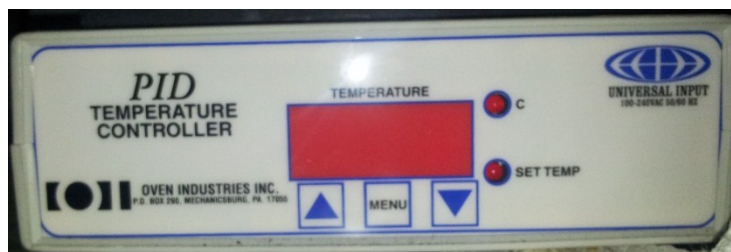


Figure 25. Evaporator Power Supply and Temperature Control.

3.3.5. Exhaust Setup

Exhaust from the growth process was bubbled through water to remove as many harmful chemicals as possible, then vented through a fume hood. However, for a safer operation, a dual beaker design was developed whereby the exhaust was pumped into an empty beaker, then into the water-filled beaker, then on to the fume hood. This was to prevent any water from getting accidentally sucked back into the furnace and causing a steam blow out in the case of a pressure drop.

3.3.6. Sample Retrieval Process

Typically, samples were grown on standard-sized quartz slides. This allowed for easy removal and recovery of the NSS material, but care had to be taken to prevent accidentally scraping or damaging the sample with the retrieval stick. Additional difficulties arose when scraping the NSS material off of the sample slides with a razor blade, often due to overall non-uniformity of the growth over the substrate, leading to rips and tears in the material. Additional material could be recovered by scraping it off the furnace sidewalls with a stick with a curved scraping hook on the end, but this often damaged the samples and produced irregular patches, and scraped off a great deal of soot and other byproducts as well. Further improvements on processing and geometry of the substrate, as well as removal tools (geometrically compatible with the substrate) will improve the “sample retrieval process.”

Chapter 4

Processing Results, Characterization, and Discussion

4.1. Processing Results for Manufactured NSSs

Although chemical vapor deposition is a relatively well-understood and studied growth process, there are various variables which change during the course of experimentation, and when any time a new process is developed there is a learning curve that must be overcome before the process can be “optimized”. The following are some of the lessons and observations made during the process of developing the NSS growth regime and proved to have as much influence on the process results as any of the experimental variables.

After several trials it became increasingly apparent that the chemical reactions leading to the formation of the NSS structure existed inside a unique reaction zone, shaped like a cone. This “reaction zone” is likely very similar to the phenomena seen in combustion physics, where chemical species merge, react, and decay in a continuous flow pattern. Hence, the horizontal and vertical position of the sample substrate relative to the injection port in the reaction furnace directly influenced the deposited material. Several sample substrates could be placed end to end, and only the first two would have NSS deposition, while the third, furthest from the injection port, would often have a thin, brittle layer of black material that crumbled when touched, or nothing at all. If a sample slide was positioned in the vertical center of the chamber, it would have a heavier concentration of the bumpy textured NSS growth recorded while trying to grow

NSSs. There are several possible explanations for this observation, all which indicate that the reaction chemistry behind the formation of the NSS structure is a complex one. Further study and modeling will be required to understand this phenomenon. Although modifications in the process parameters improve the reaction chemistry, physical modifications such as a shaped injector nozzle will likely prove important as well.

Temperature stability and dynamics in the furnace also proved to be more important. The reaction tube was not fixed to the furnace, so could be slid horizontally as far as the flange fittings would allow. In addition, a dual-port feedthrough flange head was purchased, which allowed for a separate gas and liquid injection line, and more importantly had lengths of tubing welded onto the reaction side of the flange head, allowing the precursor and gasses to be injected all the way into the hottest zones of the furnace. Once it was determined that mixing and evaporation of the precursor prior to injection was vital to successful growth, a single port was used instead, which allowed more control over the distance between injection and growth zone. It was then discovered that if the precursor was injected too far into the furnace, the carbon feedstock would “crack” and leave a thin layer of graphite and amorphous carbon, or soot. Interestingly, some samples were retrieved which had an underlayer of graphite with a top layer of NSS material. Even more interesting, the graphite layer was semi-flexible, perhaps being a new “NSS + Graphite” hybrid material. As another newly discovered material, a flexible graphite would have many interesting applications, and hence would require an entirely separate line of research.

If the precursor was injected too far away from the furnace zone (if the furnace tube was pulled all the way out), the reaction would not proceed as desired, and only amorphous carbon would be deposited, or nothing at all. This may also be influenced by temperature uniformity in the

furnace tube itself; since the exposed quartz tube is not wrapped in heat tape or insulation, it will be exposed to air and will therefore have a much lower temperature than the reaction zone. If the chemical constituents do not reach the optimal growth temperature before they react, they may simply break apart into amorphous carbon or other byproducts instead of forming carbon nanotubes, or re-condense inside the tube, with similar results. It was also found that allowing the furnace temperature to stabilize for approximately 30 minutes improved the uniformity of the resulting deposited material. Gas flow simulations and chemical reaction models could further confirm these phenomena, but the experimental observations suggest that the NSS growth reaction is directly influenced by temperature gradient stability, gas flow dynamics, and proper mixing of the reacting components.

Other factors which may influence the outcome of an experiment are the cleanliness of the substrate and the sonication time for the precursor solution. As for the importance of a clean substrate, although a clean substrate is preferable, it does not appear to be a determining factor. Another interesting factor to consider is that the depositing layers of NSS material can change the heat transfer characteristics of the furnace tube sidewalls, and hence can influence the rate of deposition over time.

It is also worth mentioning that the most effective method for cleaning the furnace tube was found to be simply opening both ends and bringing the furnace above 600°C, at which point all the carbon would burn off. A clumped paper towel could then be pushed through, removing the remaining iron powder residue.

4.2. Characterization Results of NSS

4.2.1. Scanning Electron Microscopy (SEM)

For the SEM studies, samples were mounted with double-stick conductive carbon tape on aluminum stubs, then imaged with a Hitachi S-4800 Field Emission Scanning Electron Microscope (FE-SEM) at an accelerating voltage of 15 kV, with a typical working distance of 10 mm.

The FE-SEM is a very powerful tool and perhaps the best way for imaging and understanding nanomaterials. The NSS material proved to be easy for imaging due to its conductivity and stability under vacuum. Although the main purpose of SEM imaging was simply to confirm the morphology of the NSS structure and compare it with the prior nanosponge work, many novel and interesting structures were observed which may provide interesting future research materials such as a unique and beautiful growth of iron crystals (see Figure 26). More importantly, some new attributes or features of the NSS material were observed, such as a distinct difference between growth phases. It was observed, when handling the material, that a top “skin” could be peeled off yielding some spongepaper samples, which looked closer to the original discovery material. These samples were brought in for imaging, and it was discovered that there is a distinct transition between phases in the NSS infrastructure and the top layer could be described as sponge “paper” NSS, with higher density and greater directional order, while the thicker underlayer could be described as the “bulk” NSS (see Figure 27), having higher porosity and a greater degree of disorder.

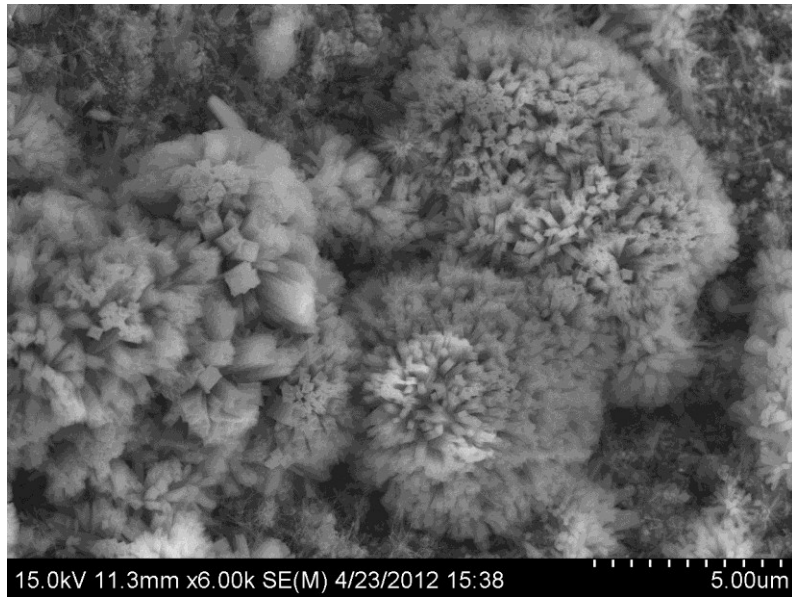


Figure 26. A unique and unexpected growth of "iron" crystals.



Figure 27. Transition between sponge "bulk" NSS and sponge "paper" NSS phases, indicating growth process may be nonlinear.

Although the NSS material proved rather simple to image, the individual nanotubes themselves proved rather more difficult, since they were so non-uniform and the depth of field kept changing. Still, enough detail could be discerned to get a sense of the quality of the nanotubes themselves. As seen below, they are most likely multi-walled, with some defects and mechanical kinks, and display both branches and fused sections. It is interesting to point out that while most research groups are attempting to grow nanotubes as uniformly as possible, the NSS structure does not require this feature and poses an array of unique features (see Figure 28 and Figure 29).

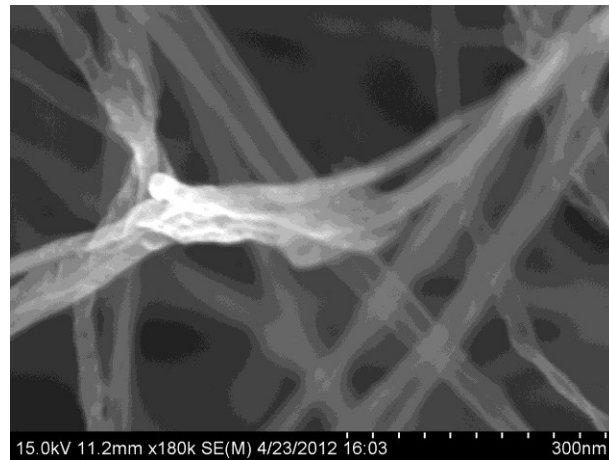


Figure 28. SEM image showing cross-linking between nanotubes, as well as kinks, bends, and other unique features.

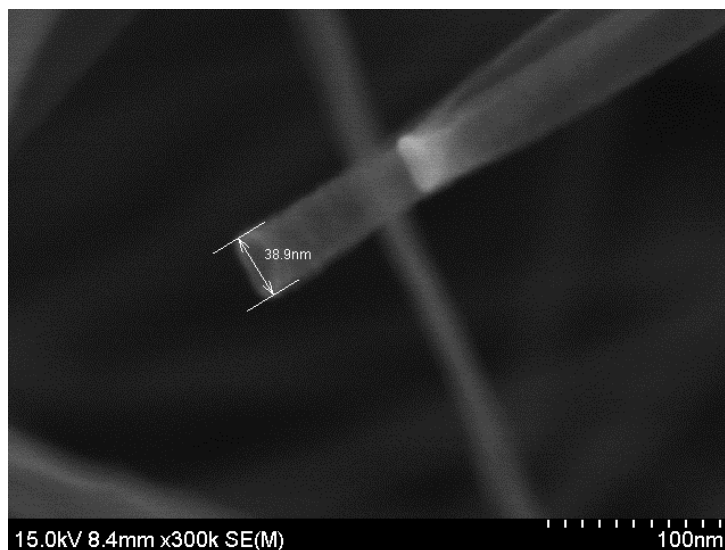


Figure 29. Close-up image of an open nanotube end, with a scale bar showing the approximate diameter at 40nm, indicating that the nanotube is multi-walled.

4.2.2. Transmission Electron Microscopy (TEM)

Transmission electron microscopy was used for imaging smaller features not visible under SEM, and for confirming the multi-walled nature of the nanotubes. Samples were first scraped onto carbon-coated lacey Formvar grids. The grids were then viewed and photographed in a Hitachi HT7700 Transmission Electron Microscope operating at 100kV with an AMT XR41 4 megapixel camera (Advanced Microscopy Techniques, Corp). Two startling and unexpected features were immediately observed-the first being that some of the nanotubes were filled with iron left over from the ferrocene catalyst (see Figure 30). The exact nature of the growth mechanism is most likely either tip-growth or base growth [46], or even a combination of the two, but it is unclear how the catalyst could get trapped inside a growing nanotube. It also appears that the iron filling seems to have an effect on the diameter of the nanotube; although the mechanism responsible for this is unclear, it is most likely some form of molecular adhesion.

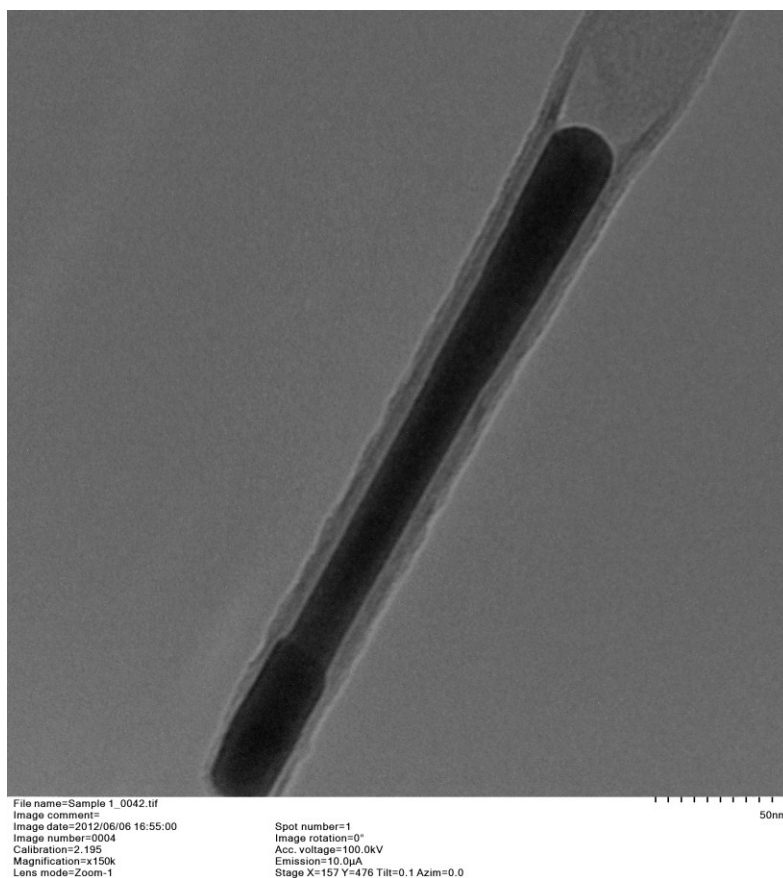


Figure 30. Carbon nanotube partially filled with iron.

The second startling observation was that many of the nanotubes seemed to be coated with non-uniform layers of amorphous carbon (see Figure 32 and Figure 33). This made it very difficult to accurately discern the number of multi-walls present for each nanotube. The cause of this coating will be investigated in future work, as will its effect on the properties of the NSS material. Figure 33 shows a combination case of carbon nanotubes with iron filling and carbon coating.

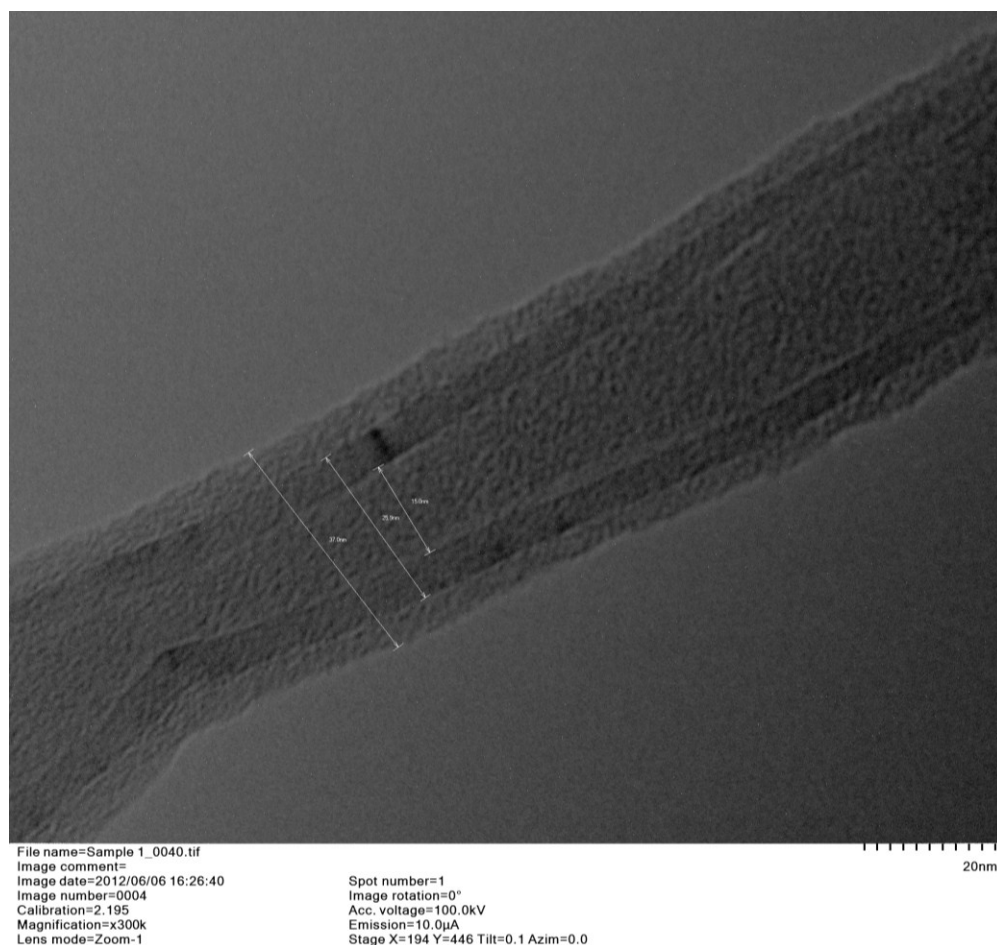


Figure 31. Carbon coated nanotube. Inner diameter is measured at 15 nm, the outer diameter at 26 nm, and the coating at 37 nm, indicating a 5.5 nm thick coating (TEM).

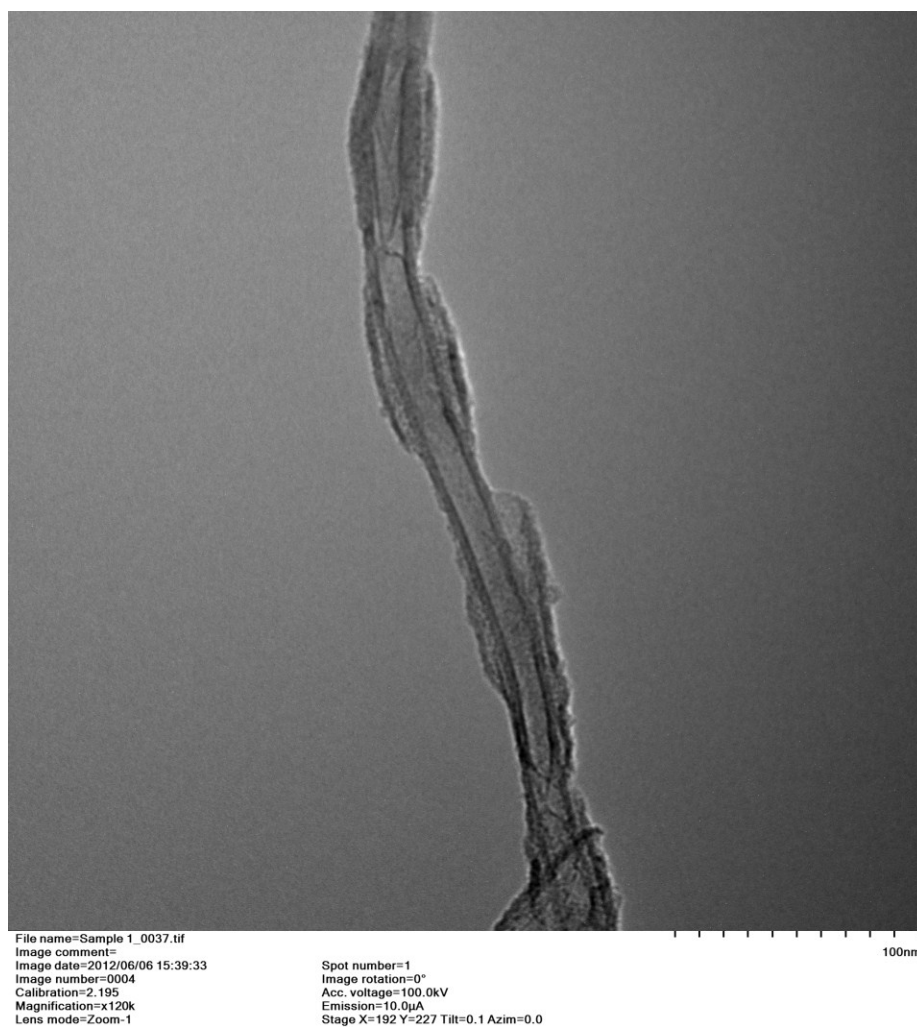


Figure 32. Carbon nanotube with irregular carbon coating (TEM).

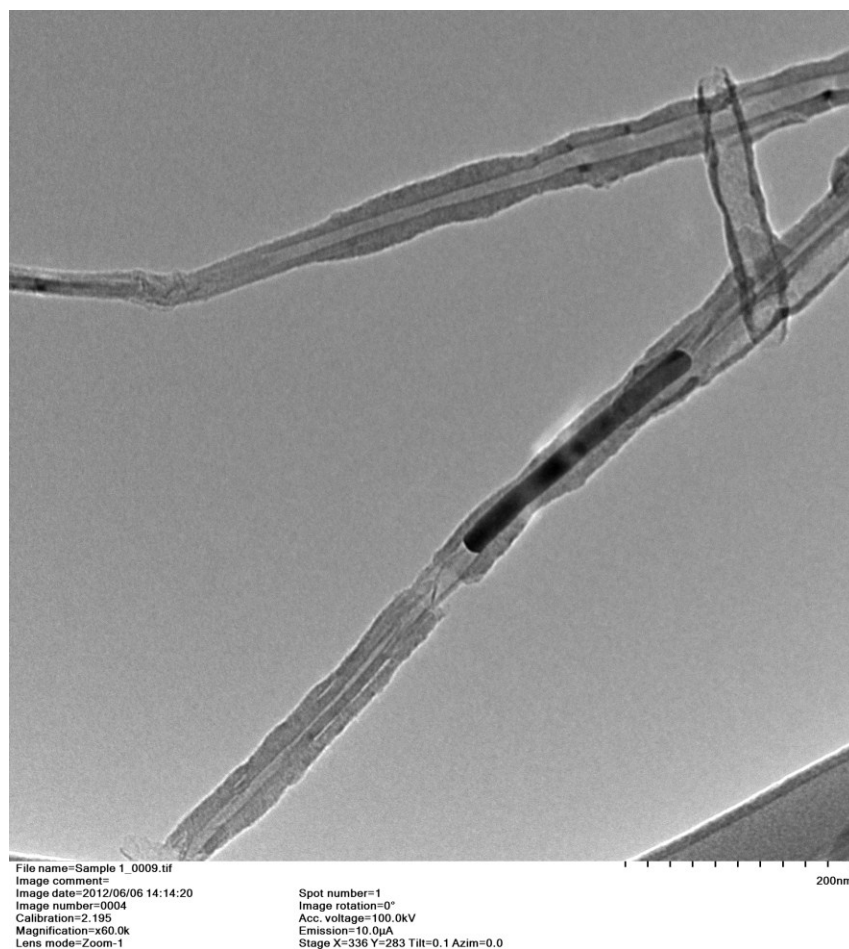


Figure 33. Nanotubes showing irregular coatings and embedded iron cores (TEM).

It will be interesting to observe the effects of an improved growth process on the relative cleanliness and uniformity of these nanotubes and their coatings, as well as any further post-processing experiments. A novel functionalization can incorporate these irregular carbon coatings, which could lead to useful technological features and applications.

4.2.3. Raman Spectroscopy

NSS sample spectra were taken with a 785 nm excitation wavelength using a Kaiser Optical Systems microRaman system. The system is comprised of a 785 nm Invictus diode laser, a Leica microscope with imaging capabilities, a Kaiser Holospec spectrometer, and an Andor CCD

camera. A filtered 50 μm optical fiber was used to transmit laser light to the microscope and the Raman signal to the spectrometer. Laser light was focused and the signal was connected through a 50X objective mounted on the microscope in a backscattering geometry, yielding a laser spot size of 4 μm on the sample. Typical acquisition time was 60s, and laser output was limited to 4mW to minimize damages to the sample.

As shown in the spectrograph in Figure 34, peaks were identified around 1300, 1600, 2600 cm^{-1} , indicating the presence of graphitic structures, which are cited in literature at 1370 and 1583 cm^{-1} [47]. The peak at 2600 cm^{-1} is known to be a reflection of the first peak, and is therefore ignored. This data shows that the NSS sample contains nanotubes, but cannot determine the type or chirality. Future work will require a range of laser wavelengths, which will be able to reveal different aspects of the analyzed nanotube samples. It is worth noting that the original sponge samples showed similar peaks, but were unable to handle to the same laser power, and showed heat damage after each run. This typically indicates a larger proportion of amorphous carbon present in the samples.

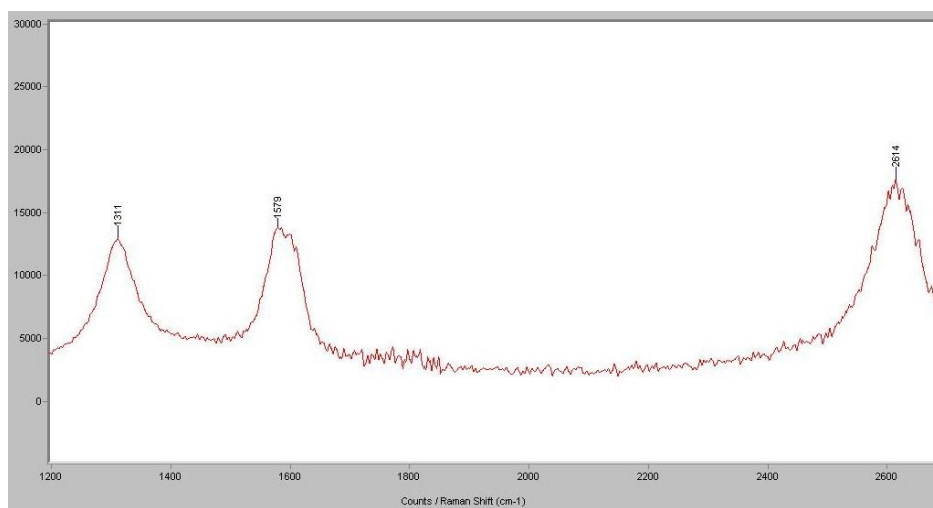


Figure 34. Raman Spectrograph of NSS sample showing peaks around 1300, 1600, and 2600 cm^{-1} .

4.3. Discussion

Although the nanosponge sheets (NSSs) have proved relatively simple and easy to characterize, they have shown there is much more yet to be discovered and studied. While there exists a great deal of literature on the physics and chemistry behind the growth and properties of carbon nanotubes which may shed some light on certain issues and answer some questions, this process and the nanosponge sheets are novel enough that a new study will be required to fully understand this process, as it is very different from conventional carbon nanotube and nanosponge growth processes. Scanning electron microscopy has shown that the nanosponge sheet morphology is similar to the structures reported by Gui et al. [33], and even similar to Ajayan et al. [34], yet still substantially different enough to be considered novel, due in large part to the long-range order of CNTs and extreme flexibility, toughness, uniformity, and cohesiveness. Further investigation has shown that there may exist two or more different NSS morphologies, based on relative density and alignment, tentatively called the “bulk” NSS and “paper” NSS phases. The exact causes of these different phases remains to be determined, but are primarily due to mixing or gas phase separation of the evaporated gas phase carbon feedstocks xylene and dichlorobenzene, which are both solvents with similar chemical structures, but different miscibility. Varying the ratios of these feedstocks is a crucial factor in controlling the properties and morphology of the resulting NSS products.

Another unexpected result from TEM observations is the presence of irregular carbon coatings on the nanotubes themselves. With greater understanding and control of the process this unexpected result can become a useful function.

The iron cores left inside some of the nanotubes is another observed and interesting feature of our NSSs, which could affect the overall properties of the nanosponge sheets. Should the

nanosponge sheets be utilized as electrical conductors or magnetic shielding materials, the iron cores could prove quite useful.

The results of the Raman spectroscopy study show that graphitic fullerenes are present, although the types and chirality remain to be seen. A spectrometer with a higher wavelength laser source could provide further information. It was also noticed that the original sponge samples were far more sensitive to heat damage from the laser, indicating a much higher percentage of amorphous carbon present in the samples.

Chapter 5

Performance Evaluations, Densification, and Functionalization

5.1. Introduction

A comprehensive study of the properties of the nanosponge sheets (NSSs) is outside the scope of this project. The process currently used to grow the material still needs improvements and, e.g., cannot yet produce samples large enough for standard mechanical tests. Still, simple handling of the material reveals its remarkable flexibility and toughness, where samples can be folded and compressed repeatedly like thin strips of foam, and will always return back to their original shape. Of course, more uniform samples display greater strength, and interestingly enough much thicker samples (e.g., about 5mm) became increasingly brittle and prone to cracking, unless they undergo a densification process explained later in this chapter.

Since proper mechanical testing will rely on consistent sample thickness, and quality with larger sizes, it will be performed during future studies. However, a number of experiments have been performed to obtain a basic understanding of some of the interesting properties of our NSS materials, and are described in the following.

5.2. Cleaning Tests

Once initial SEM observations showed an excess of iron particulates and random debris scattered across the surface of the NSS material, it became imperative to develop methods to remove them. As one application, the functionality of the nanosponge sheets as a fuel cell gas diffusion

or catalyst layer might be diminished if the iron particles interfered with the chemical reactions of the fuel cell. It is important to note that the residual iron catalyst clusters and random surface debris were found only on the surface side of the NSS samples, and the infrastructure and bottom of the samples were found to be clean and particulates-free.

5.2.1. Sonication in Ethanol

A small sample of nanosponge sheet was placed in a vial and immersed in ethanol, and then placed in a sonicating bath. Almost immediately, the sample began deteriorating into clumps. The core sample did not break down immediately, but instead gradually decomposed around the exterior. After 5 minutes, the vial was removed, and some of the loosened material was spread onto carbon tape and imaged via SEM. While the sonication in ethanol disintegrates the spongepaper infrastructure to some extent, it did remove the particulates and iron clusters, as shown in Figure 35.

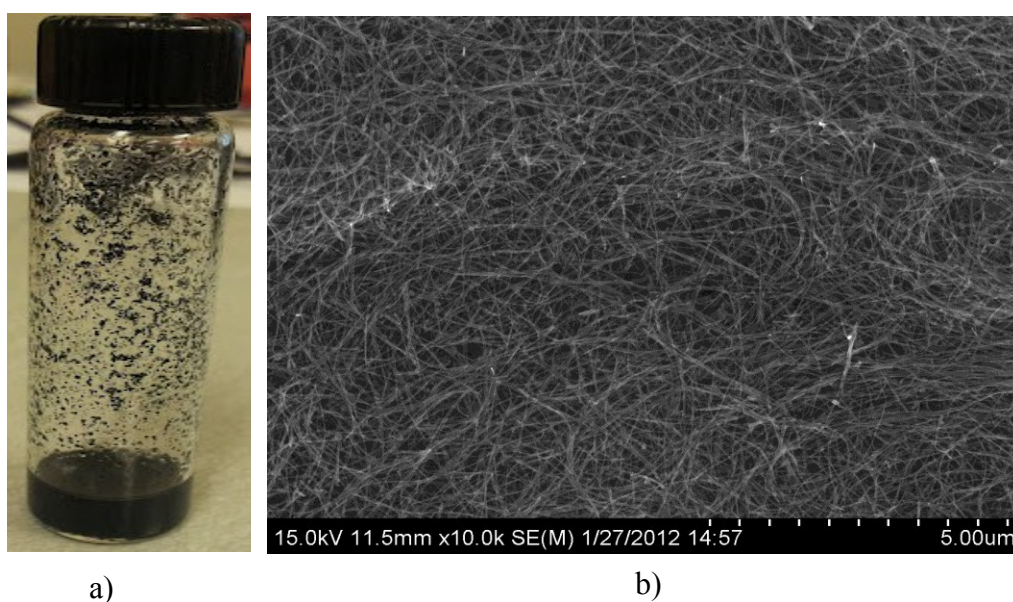


Figure 35. a) NSS sample after sonication in ethanol for 5 minutes, b) SEM image showing removal of contaminants.

Although sonication has been shown to be impractical for bulk cleaning of the nanosponge paper material when the preservation of the infrastructure is desired, it may prove to be a useful technique should the need arise for producing large quantities of bulk, disordered nanotubes as a filler material. Further imaging of the sonicated NSSs in ethanol for 5 minutes shows total deterioration of the NSS (see Figure 36); however, no damages to individual CNTs were observed (see Figure 37).

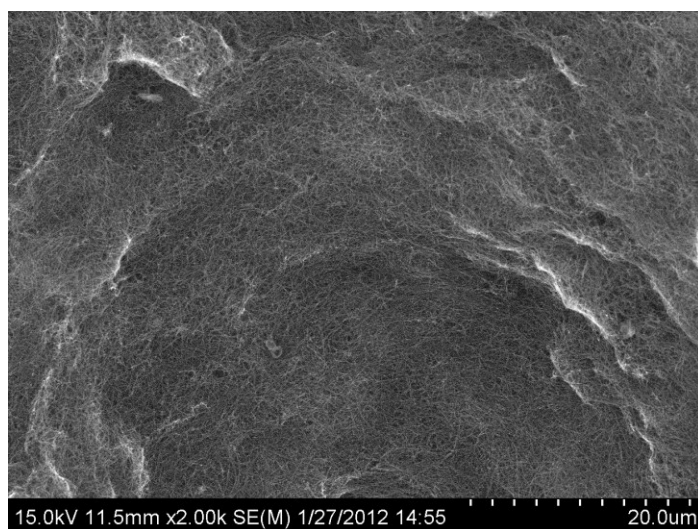


Figure 36. Further imaging of sonicated NSS material, showing total deterioration of the ordered NSS infrastructure (SEM).

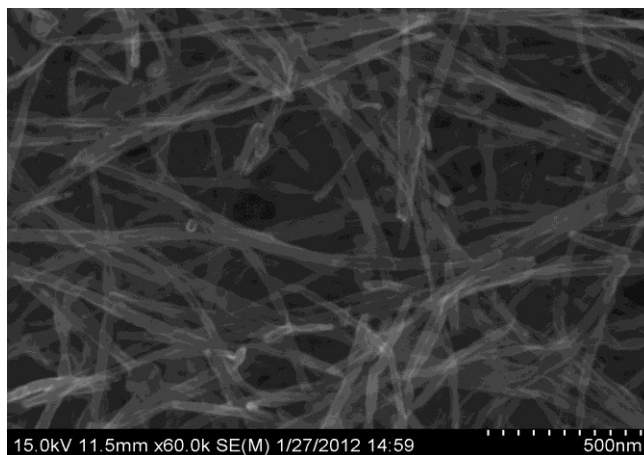


Figure 37. Higher magnification image of ethanol sonicated NSS sample (for 5 minutes), showing no damage to individual nanotubes (SEM).

5.2.2. Flame Test

In another attempt to remove the iron particulates and other contaminants, a different approach was taken. The sample was soaked in acetone, which it absorbed instantly, and then ignited. A large flame was observed coming off the NSS sample for approximately 30 seconds (see Figure 38), as the sample gradually shriveled up, but did not burn (see Figure 39). Instantly after the flame died out, the sample expanded back to its original shape, and could be immediately picked up and handled with no deterioration or damage (see Figure 40). This test could be repeated numerous times on the same NSS sample, with only minor degradation due to oxidation at the edges of the sample. This became known as the “flame test” and was demonstrated to tour groups, sometimes using the same sample around 15 times over the course of a day.

However, when the fresh NSS (i.e., without any acetone) was exposed to an open flame, it immediately burned off. A likely explanation for this phenomenon is that the acetone coated the individual nanotubes and protected them from the oxygen in the air, allowing the heat to burn the acetone instead of the nanotubes. This experiment also demonstrates the extraordinary thermal conductivity of the nanosponge sheet, especially since the samples could be handled immediately

after the flame test without the slightest discomfort in terms of heat and temperature. Given its flexibility and compressibility, the NSS material would likely make an excellent candidate for the next generation of heat sinks, particularly for thermal management of electronics and advanced systems.



Figure 38. NSS sample undergoing "flame test".



Figure 39. NSS sample shriveling near the end of the flame test, as trapped acetone is burned away.

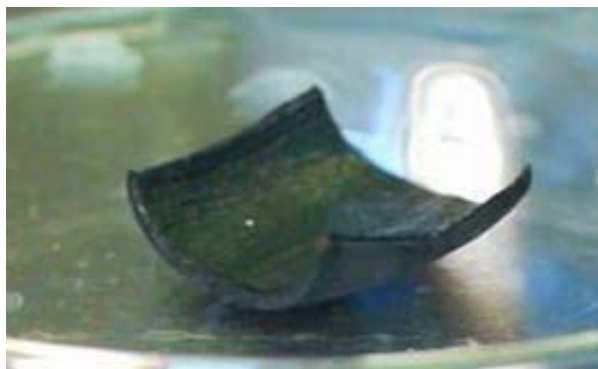


Figure 40. NSS sample resumes its original shape immediately after the flame test, and can be handled without discomfort in terms of heat and temperature.

SEM imaging of a burnt section of the NSS sample (at the edges) revealed some unusual formations resulting from the flame test, including another unique crystal structure of iron catalyst clusters (see Figure 41). The most dramatic changes to the NSS infrastructure after burning at the edges appears to have specifically affected the iron catalyst clusters, fusing them into larger crystalline sections, while leaving the rest of the nanotube infrastructure relatively intact (see Figure 42).

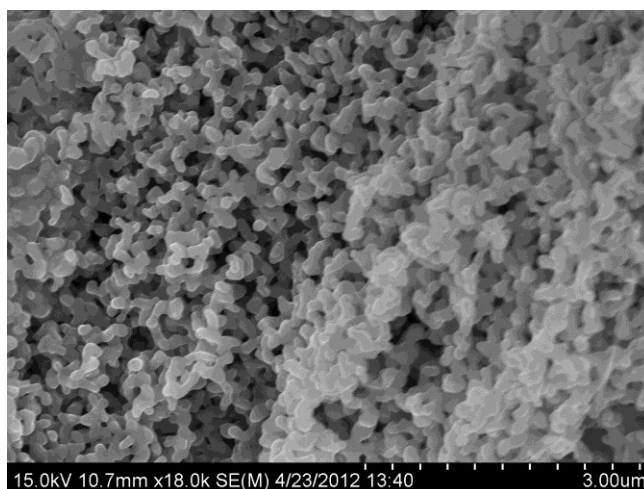


Figure 41. SEM image of NSS sample after flame test, showing unique iron catalyst crystal formations.

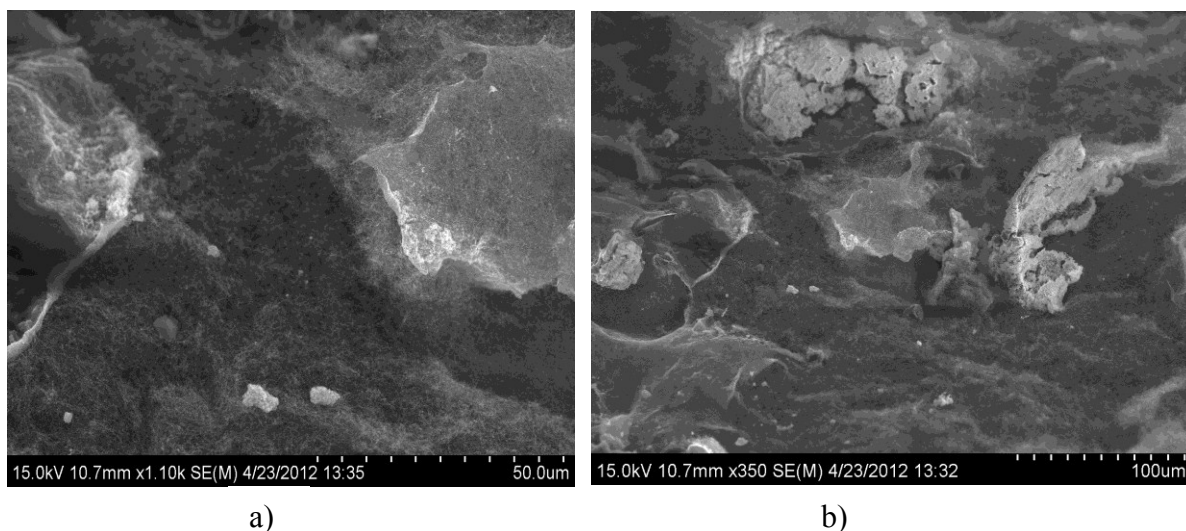


Figure 42. SEM images of a) the NSS surface after flame test (at the edges), b) fused clusters of metallic catalyst, with apparently undamaged nanotube infrastructure left intact.

5.3. Densification

Another interesting result was observed while conducting some thermal properties tests, which has led to a process now described as “densification”. Pristine (as-manufactured) NSS samples are hydrophobic, but can be partially wetted by squeezing them while submerged in water. This partially wetted sponge sample is then placed on a hot plate, heated to over 100°C. The water immediately evaporates and boils off, including any water that is trapped inside the NSS infrastructure. This has the effect of removing nearly all the air trapped inside the NSS infrastructure as well, which causes the NSS to shrivel and condense from a foam-like structure of about 1 mm in thickness into a flat, paper-like piece of 35 microns in thickness, indicating a 96% porosity for the NSS. This process will apparently change the surface energy of the sample, as once it is re-submerged in water it will expand into its original shape, with somewhat reduced hydrophobicity. SEM imaging confirms the densification theory (see Figure 43), showing a surface with dramatically reduced pore sizes and flattened features.

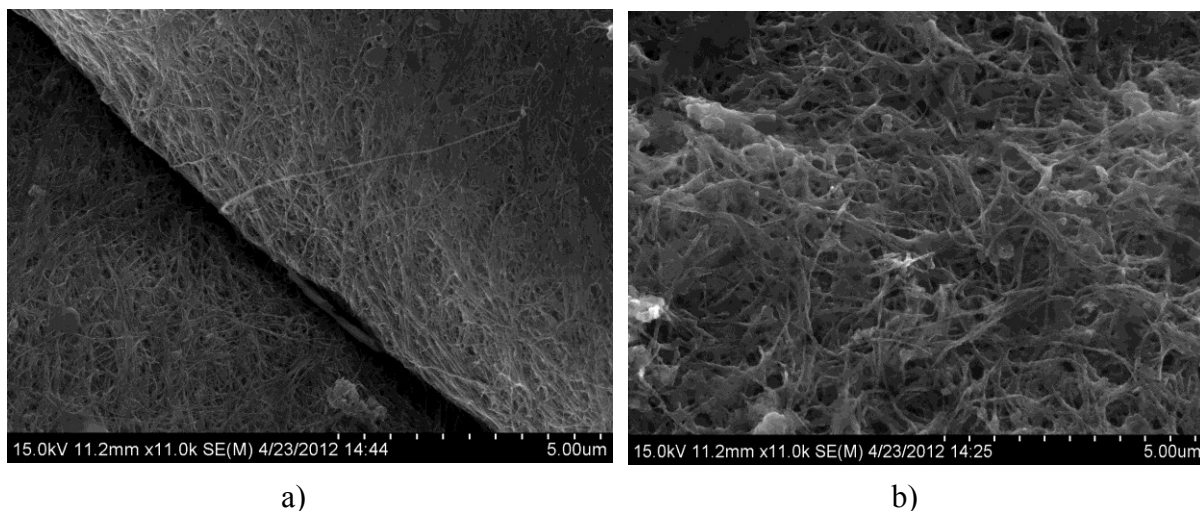


Figure 43. SEM images of a) densified NSS sample, showing compressed layers of nanotubes, and b) reduced pore sizes (large features, such as creases and curves, are still preserved).

Densified samples were close approximations of the original NSS material discovery, despite having higher density and reduced porosity. Their surfaces were still flexible enough to show depressions and contours made by forceps, and were measured to have a thickness of approximately 35 μm (see Figure 44). Considering the original samples were approximately 1mm thick, the densification reduced the sample thickness by three orders of magnitude, using a reversible process with minimal sample damage and without the need for chemical treatments. This “densification” process may prove to be one of the more useful structural alteration techniques for the NSS materials.

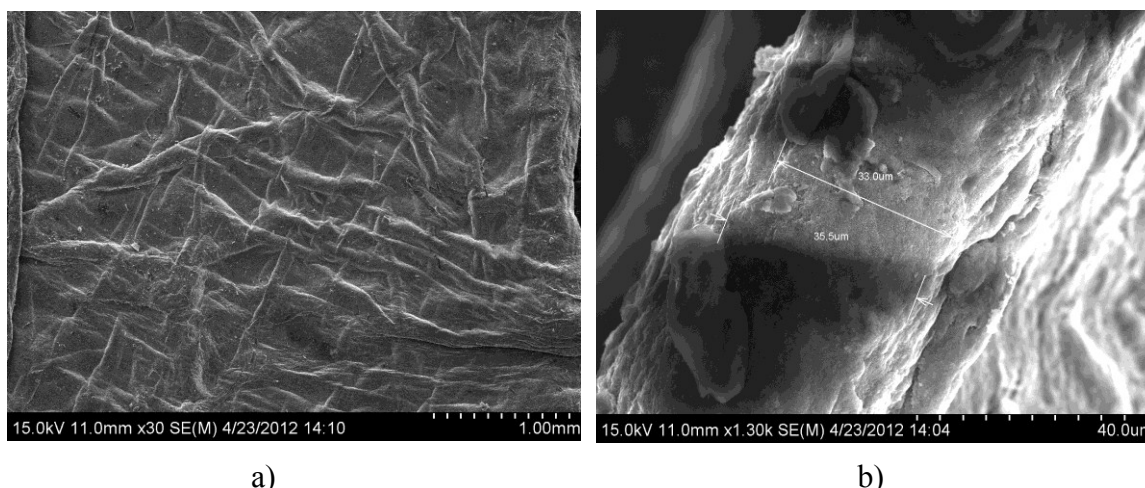


Figure 44. SEM images of a) densified NSS showing surface impressions left by forcep tweezer grips, and b) measured sample thickness of approximately 35 microns.

5.4. Acid Treatment Functionalization

Prior work has demonstrated that carbon nanotubes treated with acid undergo sidewall etching and defects, which can alter their magnetic and chemical properties [48]. For this experiment, the goal was to apply acid treatments functionalization from prior studies, and convert the hydrophobicity nature of pristine Nano-Sponge Sheets to hydrophilic nature. As mentioned earlier the as-manufactured NSS is hydrophobic and when placed in a container of water it floats. Further, NSS samples were immersed in a solution of nitric and sulfuric acids at a ratio of 1:3 for 1 hour. Samples were then placed into a container of water, where they immediately sank to the bottom, indicating total hydrophilicity (see Figure 45). The experiment was then repeated, reducing the acid exposure time, and it was found that only 10 seconds of acid exposure was necessary to alter the properties of the sample from hydrophobicity to hydrophilicity. Even more interesting, exposing the samples for less than 10 seconds made the sample partially hydrophilic (and partially hydrophobic), where the NSS is suspended in a container of water, indicating that the hydrophobicity/hydrophilicity of the NSS is “tunable” (see Figure 45). This feature has broad

implications for future work with other applications, and opens up a whole range of possible chemical treatments and applications that may not have been possible before.

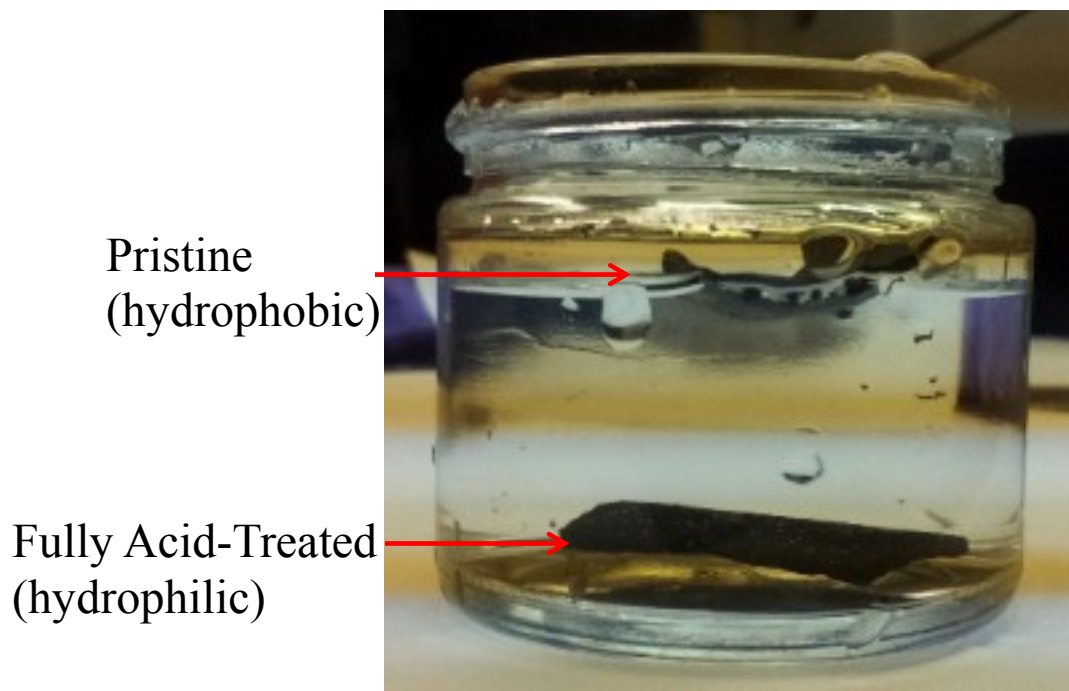


Figure 45. Tunable functionalization on hydrophobicity/hydrophilicity of the NSSs employing acid treatment.

SEM imaging of acid-treated samples revealed apparent roughening of the individual nanotubes (with potential creation of defects as well as carboxyl, hydroxyl, and epoxide groups), which accounts for the change in surface energy (see Figure 46).

It should be noted that the above-mentioned tunable functionalization technique could also serve as a “cleaning process” for the developed NSSs.

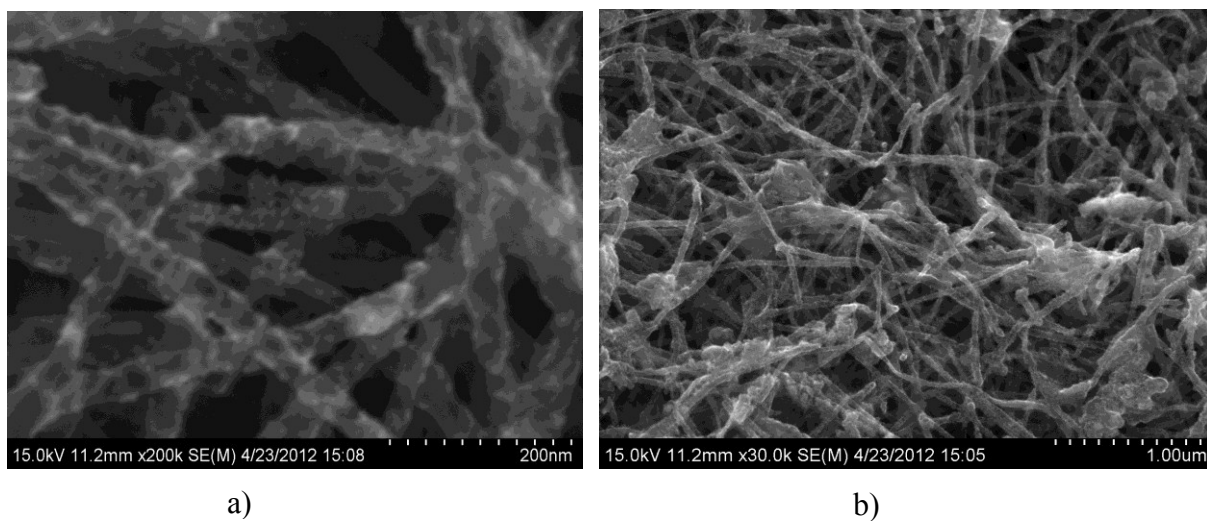


Figure 46. a) Acid-treated NSS samples showing rougher nanotubes at high magnification and b) lower magnification.

Chapter 6

Preliminary Applications

6.1. Introduction

Carbon nanotubes have proven to be highly adaptable materials with applications in a wide range of functions and industries. As stated earlier, their nanoscale size which enables such remarkable properties has also rendered them extremely difficult to work with, and hence severely limited the type and degree of practical applications possible. The nanostructured nanosponge sheets has proven to be a highly attractive variant of the carbon nanotube material for macroscale applications, and is expected to lead to a number of useful developments. For this research, a few basic applications were explored, as explained in prior chapters as well as this one.

6.2. Fuel Cell Applications of NSSs

To test the viability of the NSS material as a potential fuel cell gas diffusion layer, two samples were first cut down to 5 sq. cm, to function as gas diffusion layers in a standard proton exchange membrane (PEM) fuel cell test setup. A catalyst coated membrane was used from prior experiments, which was a Nafion® NRE-211 membrane (Ion Power Inc, New Castle, DE), spray-coated with a platinum/carbon slurry and a 15 wt% Nafion® solution (Ion Power Inc, New Castle, DE). The NSS gas diffusion layers and the catalyst coated membrane were assembled in a single test cell (Fuel Cell Technologies, Albuquerque, NM, USA) by sandwiching them together with silicone-coated fabric (CF1007, Saint-Gobain Performace Plastics) to provide gas sealing. The cell was closed and tightened to a uniform torque of 40 lb-in. The cell performance was tested using galvanostatic polarization with Greenlight Test Station (G50 Fuel cell system,

Hydrogenics, Vancouver, Canada). The cell was purged with nitrogen and tested at 70°C with H₂/O₂. Hydrogen gas was flowed over the anode at a rate of 0.2 SCCM and oxygen was flowed over the cathode at a rate of 0.4 SCCM. The humidity in the cell was controlled by adjusting the humidity bottle temperature. The resulting voltages were recorded, and the waste water was collected in a tub. Further tests were conducted with decreasing humidity. An ideal goal would be to have optimal performance at a relative humidity close to ambient air atmospheric conditions, essentially allowing the fuel cell to operate on air.

Despite being much thicker than the standard carbon paper gas diffusion layer, the NSS membranes actually performed much better, and maintained their power density at decreased humidity. Still, carbon paper with pressed-on or as-grown nanoforest carbon nanotubes were able to achieve an even higher power density (see Figure 47), but NSS reached its stable asymptotic performance faster over a wide range of relative humidity. Future work with fuel cell membranes will focus on making thinner and more porous NSS samples, to increase the molecular transport kinetics needed for improved fuel cell functions as fuel cell gas diffusion layers (GDLs). The reason the CNT-based GDLs perform better than standard carbon papers (SCPs) is that SCPs are hydrophilic and absorb the moisture that is in fact provided for the Nafion to function properly, while NSSs are hydrophobic and repel the moisture, thus improving the performance (power density) of the fuel cells, reducing the needs for relative humidity, and improving the life of NST-based GDLs, since when the SCP-based GDLs absorb moisture, they degrade in performance in time.

Further, the NSS can be loaded by a thin (nano-level) coat of platinum (also see next section on sputter coating) or platinum nanoparticles to function as Catalyst Layers (CLs) in PEM fuel cells.

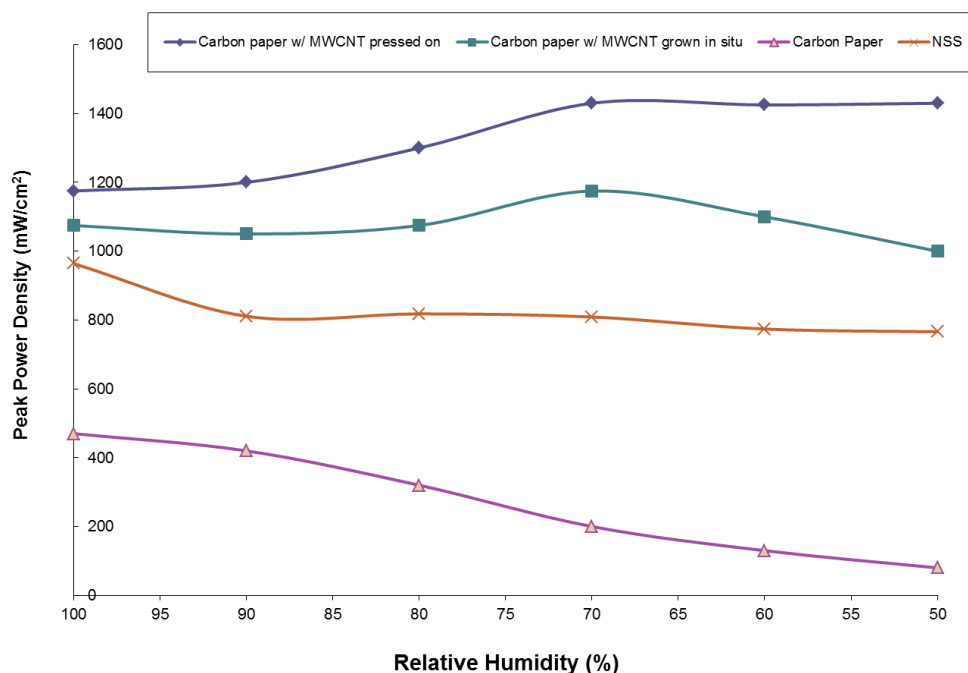


Figure 47. Peak Power Density vs Relative Humidity. NSS GDLs perform better than standard carbon papers, but less than carbon paper enhanced by MWCNTs-based nanoforests.

6.2.1. Sputter Coating

Future applications involving nanosponge sheets will require alterations of the materials conductivity and surface reactivity. Sputter coating is a well-understood and widely used method for depositing an atomically thin layer of metal onto the surface of a substrate, typically to increase its conductivity [49]. For example, biological SEM samples are not conductive and must be sputter coated with a thin layer of metal or conductive carbon prior to imaging, to prevent charge buildup.

Prior to imaging, a nanosponge sheet sample was sputter coated with approximately 2nm of gold/palladium using a Hummer 6.2 sputter coater, from Anatech LTD (see Figure 48).

The resulting images show excellent uniform coverage, with deposited metal islands approximately 10 nm in diameter deposited across the first few levels of the infrastructure (see

Figure 49 and Figure 50). Sputter coating is clearly a surface treatment, functionalizing the entire NSS infrastructure will require an entirely different approach, and will likely require wet chemistry (such as platinum nanoparticles loading of the NSS for PEM fuel cells catalyst layer application mentioned in the previous section). Still, the sputter coating technique is relatively quick and easy, and very effective. With a range of sputtering targets available, there is a wide variety of potential applications that become viable for the nanosponge sheet material.



Figure 48. Sputter coating a gold/palladium layer on a NSS sample.

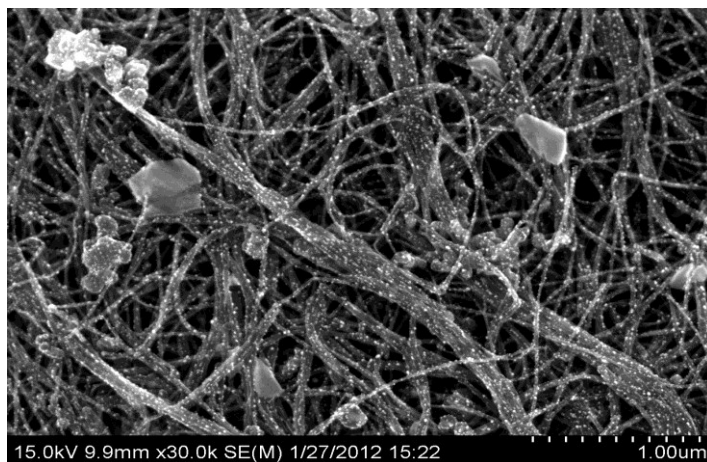


Figure 49. NSS surface sputter coated with Au/Pd.

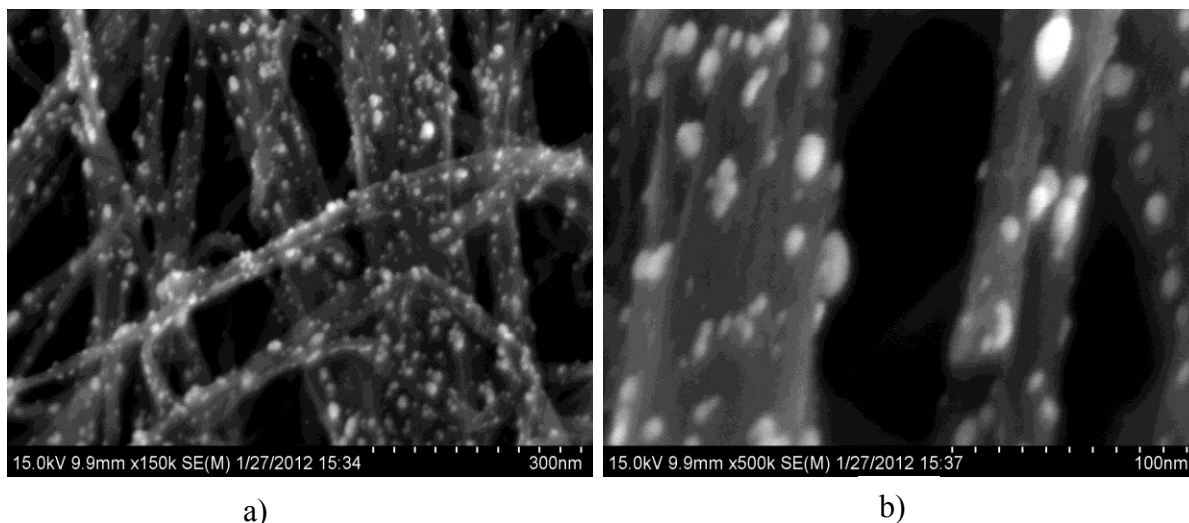


Figure 50. a) Higher magnification images of deposited Au/Pd island sputter coated on the NSS surface, b) Individual metal islands are approximately 10-20 nm in diameter.

6.3. Composites

The porous infrastructure of the nanosponge sheet material makes it an obvious candidate for composites applications. Prior work involving carbon nanotubes in composites have used them as additives, with relatively low concentrations and shortened nanotubes yielding superior results [50]. This line of research has shown great promise, and will continue to create new and interesting improvements [51]. The NSS material performs a different role as a composite- since it is interconnected and free-standing, it is not an additive, but the CNTs of the NSSs function as the primary structural reinforcement similar to the carbon fibers in Carbon-Fiber Reinforced Polymer (CFRP) composites.

To test the capacity of the NSS material as the primary reinforcement for composites, an EPON epoxy resin was chosen. The resin was enhanced with graphene platelets (xGnP grade C, manufactured by XG sciences) at 0.03 % by weight. The resin was heated till a low viscosity liquid was obtained, then incorporated into the NSS infrastructure via vacuum filtration.

Unfortunately, several issues arose-the NSS sample was not large enough, and so a great deal of resin was pulled through without infiltrating the sample. Also, the resin was still too viscous to

flow through correctly and had to be thinned out with acetone. As a result, the composite sample was not uniformly infiltrated, and hence the pools of resin cured unevenly on the sample surface (see Figure 51).

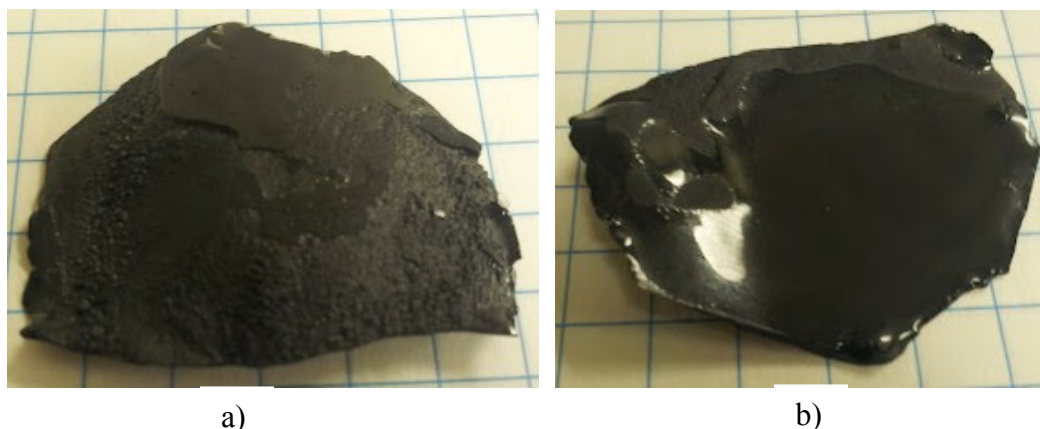


Figure 51. a) Bottom and b) top of composite sample, showing cured pool of resin, with shiny top surface and rougher underside.

After infiltration, the resin was cured with a 2 stage cure cycle: 2 hours at 40°C, then 2 hours at 100°C, then 3 hours cool-down. The resulting composite showed complete, if imperfect infiltration, and was hard and somewhat brittle. Even more surprising, the composite surface was electrically conductive, whereas the resin itself, despite being enhanced with graphene platelets, was known to be non-conductive.

SEM imaging revealed that the graphene platelets were unable to infiltrate the NSS infrastructure, and were thus left filtered on the sample surface and potentially contributed to the surface conductivity. The resulting images are very interesting, showing three different phases of material-the resin, the platelets, and the underlying NSS nanotube network (see Figure 52).

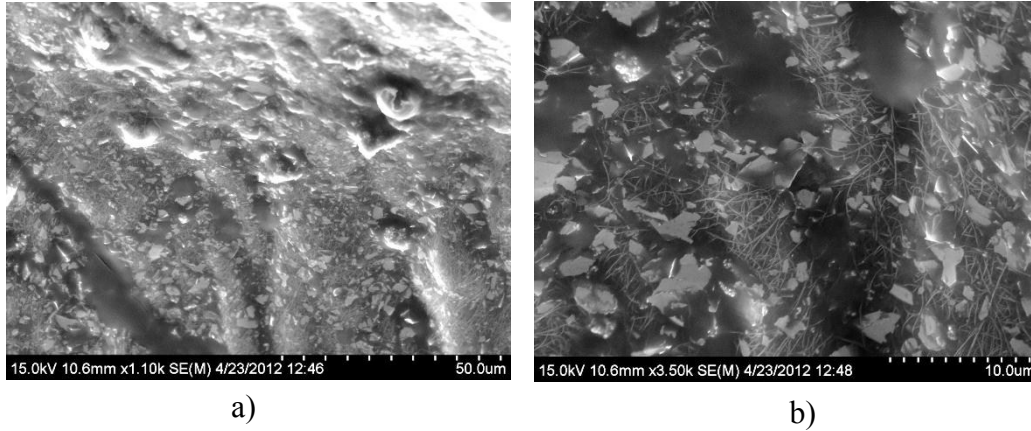


Figure 52. SEM images of composite surface, showing a) pools of resin (black), with distributed graphene platelets (gray) and b) underlying nanotube network (continuous lines).

In addition, the produced composite using our NSS was tested using a magnetic field and proved to have magnetic properties, attributed to the iron filled CNTs of the NSS (see Figure 53).

Future work on composites will obviously require fixing the many problems in the infiltration procedure, such as reducing the viscosity of the resin, ensuring a proper vacuum seal on the sample, and removing any unnecessary additives too large to pass the NSS pores. Despite its initial shortcomings, this test proved to illustrate the capacity of the NSS infrastructure as a great primary reinforcement potential for future composites.



Figure 53. TEM image showing nanotube partially filled with iron.

Chapter 7

Potential Applications

7.1. Introduction

Carbon nanotubes are already being utilized and developed in a wide range of applications, and have been considered promising candidates for many more. NanoSponge Sheets (NSSs), being a macroscale structure composed entirely of as-grown carbon nanotubes with matching nanoscale properties, flexibility, and structural integrity will likely find many more applications in line with conventional nanotube research, and many new ones.

At present, carbon nanotube nanosponge sheets display a range of interesting properties, each of which may lead to valuable future applications. These properties include: high thermal conductivity, electrical conductivity, compressibility, high strength and flexibility, high surface area/porosity, and controllable hydrophobicity. A number of the experiments described in this research demonstrate that many current applications already exist, such as the flame test, tunable hydrophobicity/hydrophilicity test, fuel cell test, compressibility test, composites test, and sputter coating test, create a clear path towards current and future development and applications possibilities. The most powerful applications of the NSS material will not be single-use; given the range of research on carbon nanotube functionalization, the NSS material will likely prove to be an ideal candidate for the next generation of multifunctional materials.

This chapter describes the range of potential applications that carbon nanotube nanosponge sheets could be employed for. Structural applications will rely on the as-grown NSS

infrastructure with minimal ex-situ modifications. Non-structural applications will require further chemical and physical functionalizations and developments, and will utilize the NSS infrastructure as the primary platform.

7.2. Structural

The first potential application utilizing the NSS infrastructure is structural composites. As shown in the previous section, the NSS material is porous enough to accept resin infiltration, and robust enough to survive the curing process. With further development of the growth process and larger CVD furnaces, larger sections of material can be grown, allowing for larger composites to be manufactured. If our method for continuously growing NSS sheets can be expanded to larger sizes, the material could be utilized much like standard carbon fiber layups, with overlapping cross-lays being impregnated with resin to form a solid shell or framework. For example, some products such as small UAVs and robots, may benefit immensely from high-strength NSS composites. Since the NSS has numerous other potential applications, it is more likely that NSS composites will be used in conjunction with other properties requirements to take advantage of its multifunctional properties. An excellent example of such applications is the lightning strike protection for aircraft, which could experience lightning strikes at least a few times per year. Aircraft with metallic skins may be able to redirect and ground out the electrical energy, but newer aircrafts with composite structures cannot readily do the same and are more susceptible to intense and sometimes catastrophic damage in the event of a lightning strike. Current solutions typically involve depositing metallic coatings on outside laminates, creating conductive paths to protect vulnerable cables and electronic components [52]. The NSS composite may prove to be a useful alternative or tool to help solve this problem, as it was shown to be conductive via surface conductivity measurements employing a multimeter. Further development will improve the

conductivity and performance of the composite, and it may eventually be used either to ground the lightning strike or help redirect the energy to other areas.

Water filtration and desalination are two separate and extremely important areas of concern in the modern world, with dwindling fresh water supplies and a rising global population exacerbating the situation. Current solutions are inefficient, expensive, labor intensive, and often environmentally detrimental [53]. Among the next generation of materials being investigated as possible solutions are metal-oxide nanoparticles, dendrimers, zeolites, and carbon nanotubes [54]. The current technologies incorporating carbon nanotubes cite toxicity and solubility as serious technical issues, requiring complex and difficult functionalization to achieve desired results. In all likelihood, a working solution will require some combination of a variety of these materials. An effective water filter and desalination membrane will require at least 3 stages: a bacteria removal medium, an organics removal medium, and a metal ions (i.e. salt) removal medium. Carbon nanotube nanosponge sheets, with a tunable porosity, adjustable hydrophobicity, and well-documented library of surface functionalization chemistry literature, may prove to be a cost-effective and robust platform for incorporating one if not all the water filtration and desalination requirements.

7.3. Non-Structural

Perhaps the most important and impactful application of the NSS material will be for energy storage and generation. This is also probably the most intensely studied and researched area of carbon nanotechnology science, and has yielded numerous papers and inventions incorporating carbon nanotubes as the next generation of cathodes for batteries and supercapacitors [55]. The main attributes of the carbon nanotube needed for this application is the conductivity and high surface area of the carbon nanotube electrode [56–59]. In addition, the high porosity and tunable

hydrophobicity/hydrophilicity of our NSS are also advantageous. Further, the same disadvantage exists for battery electrodes as for other applications when conventional carbon nanotubes are used since they are difficult to work with because of their size, and must be used in conjunction with other substrate materials. This difficulty may prove to be an enormous advantage for nanosponge sheets, since they can be grown and manipulated as free-standing macroscale structures overcoming this enormous problem. Of course, the electron transport characteristics of the currently grown nanotubes typically used in the literature should be evaluated as compared to the nanotubes grown in the nanosponge sheets to ensure the production of more electrically conductive variants of the NSS material.

Perhaps the easiest and most obvious application of the NSS material is as a thermal heat sink. The flame test has already shown the amazing ability of the NSS material to rapidly transfer heat into the atmosphere, and could prove extremely valuable as cooling units for high-end computers and electronics. Further process development will yield longer, more aligned CNT bundles in the NSS infrastructure, which will in turn allow for higher rates of thermal conductivity. Beyond basic enhancement of material properties, future development of a NSS heat sink will likely have two directions. The first direction is enhancing the thermal transport abilities of the material via functionalization with other additives, like embedded nanodiamonds or metallic coatings. The second direction, which is more long term and multifunction oriented, is to make the heat sink into a thermoelectric generator, via the thermoelectric effect. Taking advantage of the Seebeck effect and converting temperature differences into electrical current would enhance existing power generation and energy harvesting methods, where a great deal of energy is lost to thermal waste, and allow for a greatly improved scale of efficiency to be achieved [60]. A more efficient thermoelectric generator, although a seemingly minor development, would have tremendously

varied and wide-spread applications and could prove to be one of the more impactful developments for nanomaterials.

Another equally important application of the NSS material is as a fuel cell gas diffusion layer (GDL) as well as a catalyst layer (CL). As demonstrated earlier, the NSS infrastructure can function as a passable fuel cell GDL, performing better than a standard carbon paper, but lower once the carbon paper is enhanced with carbon nanotube nanoforest. The basic performance of NSS fuel cell GDLs and CLs can be further improved with intelligent growth process design of our NSS.

Another less obvious but still important potential application of the NSS material is for shielding against electromagnetic interference (EMI). Electromagnetic interference can be a problem in signal transmission in radio, wireless interlinking, and telecommunications, and an important aspect in any telecommunications technology. As prior work has shown, carbon nanotube polymer composites can make effective EMI shields [61]. A larger and denser NSS or polymer composite made out of the NSS material could enable less signal loss in standard communications technologies, meaning less power and time to be needed for amplifying and cleaning the signals. This may also become important in space communications, where solar radiation can seriously hamper satellite functions. Further uses may include shielding against radio jamming or electromagnetic attacks in the military battle space.

Chapter 8

Conclusions and Future Work

Recently discovered while trying to recreate carbon nanotube sponges as reported by Gui et al. [33] nanosponge sheets have demonstrated a number of remarkable properties which will potentially lead to a number of useful applications and discoveries in the future. While there are limited quantitative data to report thus far, the basic properties tests that have been performed so far show that this is indeed a new type of nanostructure and bulk nanomaterial, and certainly one that warrants further investigations.

The NSS material with carbon nanotube building blocks has exhibited a high degree of thermal conductivity, electrical conductivity, flexibility and durability, and high porosity with low density. It has proven compatible with resins impregnation for composites manufacturing, and has also been shown to be an acceptable target for the sputter coating of metals. Further functionalization has shown that the NSS material can be densified via forced water evaporation, or changed from hydrophobic to hydrophilic with selective acid etching. NSS layers have also been proven as functional fuel cell layers, performing better than standard carbon papers despite being much thicker. As more tests are performed, new properties and capabilities will emerge, leading to even more potential applications and discoveries.

As exciting as these developments are, a great deal of basic research and process refinement remains to properly implement NSSs as multifunctional materials for various modern nanotechnology applications.

Much of the initial work will be in improving the basic growth process, such as testing different precursor chemistries and varying the ratios of xylene, dichlorobenzene, and other carbon sources as well as additives. Although it was not reported under the results section, a test was performed where multi-walled carbon nanotubes were suspended in the precursor solution prior to injection, with the intent of having them act as nucleation sites or growth templates during the actual growth process. Unfortunately, the nanotubes were not properly suspended, and were seen to clump together during injection, yielding no noticeably different results. This is an interesting example of precursor additives which may, with proper implementation, yield entirely new and superior material results, and allow for fine-tuning of the NSS characteristics.

More future work will involve modeling the gas flows inside of the reaction furnace tube, accounting for furnace temperature and sample placement to optimize material yields. In addition, it may prove useful to obtain better injection equipment, to shape the gas flow inside the chamber in order to achieve uniform NSS coverage and more efficient use of precursor chemicals. Along these lines a sonicating injector nozzle or a sonicating attachment for the injection syringe may be used to ensure precursor uniformity, as well as aiding in any possible additives. Finally, a better method for separating the NSS samples from the quartz substrate without damaging either the sample or the substrate will be necessary. Etching the surface layer of the substrate may work, but may not prove safe and may degrade the substrates (which are expensive and must have even surfaces for the catalyst clusters to land on).

Although it was discovered by accident and as a result of a failure in producing the traditional CNT-based nanosponge, the nanosponge sheet material has the potential to be an extremely useful nanostructure platform for future nanomaterial applications and one of the first true materials capable of successfully translating nanoscale phenomena into macroscale functionality.

REFERENCES

- [1] X. Gui, H. Li, K. Wang, J. Wei, Y. Jia, Z. Li, L. Fan, A. Cao, H. Zhu, and D. Wu, "Recyclable carbon nanotube sponges for oil absorption," *Acta Materialia*, vol. 59, no. 12, pp. 4798–4804, 2011.
- [2] R. N. Kostoff, R. G. Koytcheff, and C. G. Y. Lau, "Global nanotechnology research literature overview," *Technological Forecasting and Social Change*, vol. 74, no. 9, pp. 1733–1747, Nov. 2007.
- [3] "Nanotechnology Companies." [Online]. Available: <http://www.nanotech-now.com/business.htm>. [Accessed: 14-Jun-2012].
- [4] "nanotech bubble." [Online]. Available: <http://nanotechbubble.blogspot.com/>. [Accessed: 14-Jun-2012].
- [5] "Organic Certification Leaders Calls for Ban on Nanotechnology in Certified Organic Products." [Online]. Available: http://www.organicconsumers.org/articles/article_9698.cfm. [Accessed: 14-Jun-2012].
- [6] S. Iijima, "Helical microtubules of graphitic carbon," *Nature*, vol. 354, no. 6348, pp. 56–58, Nov. 1991.
- [7] M. S. Dresselhaus, G. Dresselhaus, J. C. Charlier, and E. Hernández, "Electronic, thermal and mechanical properties of carbon nanotubes.," *Philosophical transactions. Series A, Mathematical, physical, and engineering sciences*, vol. 362, no. 1823, pp. 2065–98, Oct. 2004.
- [8] R. H. Baughman, A. A. Zakhidov, and W. A. de Heer, "Carbon nanotubes--the route toward applications.," *Science (New York, N.Y.)*, vol. 297, no. 5582, pp. 787–92, Aug. 2002.
- [9] U. Vohrer, I. Kolaric, M. . Haque, S. Roth, and U. Detlaff-Weglikowska, "Carbon nanotube sheets for the use as artificial muscles," *Carbon*, vol. 42, no. 5–6, pp. 1159–1164, Jan. 2004.
- [10] G. M. Spinks, V. Mottaghitalab, M. Bahrami-Samani, P. G. Whitten, and G. G. Wallace, "Carbon-Nanotube-Reinforced Polyaniline Fibers for High-Strength Artificial Muscles," *Advanced Materials*, vol. 18, no. 5, pp. 637–640, Mar. 2006.
- [11] P. Marks, "Nanotubes strengthen artificial muscles," *The New Scientist*, vol. 195, no. 2612, p. 28, Jul. 2007.

- [12] M. Ferrari, A. P. Lee, and L. J. Lee, Eds., *BioMEMS and Biomedical Nanotechnology*. Boston, MA: Springer US, 2006.
- [13] J. Wang, "Carbon-Nanotube Based Electrochemical Biosensors: A Review," *Electroanalysis*, vol. 17, no. 1, pp. 7–14, Jan. 2005.
- [14] H.-M. So, K. Won, Y. H. Kim, B.-K. Kim, B. H. Ryu, P. S. Na, H. Kim, and J.-O. Lee, "Single-walled carbon nanotube biosensors using aptamers as molecular recognition elements.," *Journal of the American Chemical Society*, vol. 127, no. 34, pp. 11906–7, Aug. 2005.
- [15] S. J. Tans, A. R. M. Verschueren, and C. Dekker, "Room-temperature transistor based on a single carbon nanotube," vol. 393, no. 6680, pp. 49–52, May 1998.
- [16] A. Javey, Q. Wang, A. Ural, Y. Li, and H. Dai, "Carbon Nanotube Transistor Arrays for Multistage Complementary Logic and Ring Oscillators," *Nano Letters*, vol. 2, no. 9, pp. 929–932, Sep. 2002.
- [17] A. Bachtold, P. Hadley, T. Nakanishi, and C. Dekker, "Logic circuits with carbon nanotube transistors.," *Science (New York, N.Y.)*, vol. 294, no. 5545, pp. 1317–20, Nov. 2001.
- [18] S. Li, Z. Yu, S.-F. Yen, W. C. Tang, and P. J. Burke, "Carbon Nanotube Transistor Operation at 2.6 GHz," *Nano Letters*, vol. 4, no. 4, pp. 753–756, Apr. 2004.
- [19] X. Li, X. Zhang, L. Ci, R. Shah, C. Wolfe, S. Kar, S. Talapatra, and P. M. Ajayan, "Air-assisted growth of ultra-long carbon nanotube bundles.," *Nanotechnology*, vol. 19, no. 45, p. 455609, Nov. 2008.
- [20] J. Di, D. Hu, H. Chen, Z. Yong, M. Chen, Z. Feng, Y. Zhu, and Q. Li, "Ultra-Strong, Foldable and Highly Conductive Carbon Nanotube Film.," *ACS nano*, May 2012.
- [21] D. S. Hecht, A. M. Heintz, R. Lee, L. Hu, B. Moore, C. Cucksey, and S. Risser, "High conductivity transparent carbon nanotube films deposited from superacid.," *Nanotechnology*, vol. 22, no. 7, p. 075201, Feb. 2011.
- [22] X. Lepró, M. D. Lima, and R. H. Baughman, "Spinnable carbon nanotube forests grown on thin, flexible metallic substrates," *Carbon*, vol. 48, no. 12, pp. 3621–3627, Oct. 2010.
- [23] A. E. Bogdanovich and P. D. Bradford, "Carbon nanotube yarn and 3-D braid composites. Part I: Tensile testing and mechanical properties analysis," *Composites Part A: Applied Science and Manufacturing*, vol. 41, no. 2, pp. 230–237, Feb. 2010.
- [24] X.-H. Zhong, Y.-L. Li, Y.-K. Liu, X.-H. Qiao, Y. Feng, J. Liang, J. Jin, L. Zhu, F. Hou, and J.-Y. Li, "Continuous multilayered carbon nanotube yarns.," *Advanced materials (Deerfield Beach, Fla.)*, vol. 22, no. 6, pp. 692–6, Feb. 2010.

- [25] A. E. Aliev, J. Oh, M. E. Kozlov, A. a Kuznetsov, S. Fang, A. F. Fonseca, R. Ovalle, M. D. Lima, M. H. Haque, Y. N. Gartstein, M. Zhang, A. a Zakhidov, and R. H. Baughman, "Giant-stroke, superelastic carbon nanotube aerogel muscles.," *Science (New York, N.Y.)*, vol. 323, no. 5921, pp. 1575–8, Mar. 2009.
- [26] B. Stein and N. Markovic, "Novel Carbon Nanotube / Silicon Aerogel Composites," *Materials Science*.
- [27] F. J. Maldonado-Hódar, C. Moreno-Castilla, J. Rivera-Utrilla, Y. Hanzawa, and Y. Yamada, "Catalytic Graphitization of Carbon Aerogels by Transition Metals," *Langmuir*, vol. 16, no. 9, pp. 4367–4373, May 2000.
- [28] Q. Wen, W. Qian, F. Wei, Y. Liu, G. Ning, and Q. Zhang, "CO₂-Assisted SWNT Growth on Porous Catalysts," *Chemistry of Materials*, vol. 19, no. 6, pp. 1226–1230, Mar. 2007.
- [29] M. B. Bryning, D. E. Milkie, M. F. Islam, L. a. Hough, J. M. Kikkawa, and a. G. Yodh, "Carbon Nanotube Aerogels," *Advanced Materials*, vol. 19, no. 5, pp. 661–664, Mar. 2007.
- [30] R. W. Pekala, "Carbon aerogels for electrochemical applications," *Processing*, pp. 74–80, 1998.
- [31] S. a Steiner, T. F. Baumann, J. Kong, J. H. Satcher, and M. S. Dresselhaus, "Iron-doped carbon aerogels: novel porous substrates for direct growth of carbon nanotubes.," *Langmuir : the ACS journal of surfaces and colloids*, vol. 23, no. 9, pp. 5161–6, Apr. 2007.
- [32] T. Bordjiba, M. Mohamedi, and L. H. Dao, "New Class of Carbon-Nanotube Aerogel Electrodes for Electrochemical Power Sources," *Advanced Materials*, vol. 20, no. 4, pp. 815–819, Feb. 2008.
- [33] X. Gui, J. Wei, K. Wang, A. Cao, H. Zhu, Y. Jia, Q. Shu, and D. Wu, "Carbon nanotube sponges.," *Advanced materials (Deerfield Beach, Fla.)*, vol. 22, no. 5, pp. 617–21, Feb. 2010.
- [34] D. P. Hashim, N. T. Narayanan, J. M. Romo-Herrera, D. A. Cullen, M. G. Hahm, P. Lezzi, J. R. Suttle, D. Kelkhoff, E. Muñoz-Sandoval, S. Ganguli, A. K. Roy, D. J. Smith, R. Vajtai, B. G. Sumpter, V. Meunier, H. Terrones, M. Terrones, and P. M. Ajayan, "Covalently bonded three-dimensional carbon nanotube solids via boron induced nanojunctions," *Scientific Reports*, vol. 2, Apr. 2012.
- [35] L. V. Basbanes, *Advanced Materials Research Trends*. Nova Publishers, 2007, p. 337.
- [36] C. N. R. Rao and A. K. Cheetham, "Science and technology of nanomaterials: current status and future prospects," *J. Mater. Chem.*, vol. 11, no. 12, pp. 2887–2894.

- [37] "Open Directory - Business: Materials: Nanomaterials." [Online]. Available: <http://www.dmoz.org/Business/Materials/Nanomaterials/>. [Accessed: 14-Jun-2012].
- [38] J. Chmiola and Y. Gogotsi, "Supercapacitors as Advanced Energy Storage Devices," *Journal of Power Sources*, vol. 2498, no. 2000, 2006.
- [39] G. K. Dimitrakakis, E. Tylianakis, and G. E. Froudakis, "Pillared graphene: a new 3-D network nanostructure for enhanced hydrogen storage.," *Nano letters*, vol. 8, no. 10, pp. 3166–70, Oct. 2008.
- [40] K. Wang, Y. Wang, Y. Wang, E. Hosono, and H. Zhou, "Mesoporous Carbon Nanofibers for Supercapacitor Application," *The Journal of Physical Chemistry C*, vol. 113, no. 3, pp. 1093–1097, Jan. 2009.
- [41] M. C. Gutierrez, M. J. Hortiguera, J. M. Amarilla, R. Jimenez, M. L. Ferrer, and F. delMonte, "Macroporous 3D Architectures of Self-Assembled MWCNT Surface Decorated with Pt Nanoparticles as Anodes for a Direct Methanol Fuel Cell," *Journal of Physical Chemistry C*, vol. 111, no. 15, pp. 5557–5560, Apr. 2007.
- [42] A. C. Jones and M. L. Hitchman, *Chemical Vapour Deposition: Precursors, Processes and Applications*. Royal Society of Chemistry, 7502, p. 582.
- [43] X. Msds, "3 2 Material Safety Data Sheet," vol. 3, pp. 1–6.
- [44] C. Identification, "Material Safety Data Sheet," pp. 1–5.
- [45] F. Msds, "1 2 Material Safety Data Sheet," pp. 1–5.
- [46] K. Bolton, F. Ding, and A. Rosén, "Atomistic Simulations of Catalyzed Carbon Nanotube Growth," *Journal of Nanoscience and Nanotechnology*, vol. 6, no. 5, pp. 1211–1224, May 2006.
- [47] M. S. Dresselhaus, G. Dresselhaus, R. Saito, and a. Jorio, "Raman spectroscopy of carbon nanotubes," *Physics Reports*, vol. 409, no. 2, pp. 47–99, Mar. 2005.
- [48] a. V. Ellis and B. Ingham, "Magnetic properties of multiwalled carbon nanotubes as a function of acid treatment," *Journal of Magnetism and Magnetic Materials*, vol. 302, no. 2, pp. 378–381, Jul. 2006.
- [49] L. Muscariello, F. Rosso, G. Marino, A. Giordano, M. Barbarisi, G. Cafiero, and A. Barbarisi, "A critical overview of ESEM applications in the biological field.," *Journal of cellular physiology*, vol. 205, no. 3, pp. 328–34, Dec. 2005.
- [50] P. J. F. Harris, "Carbon nanotube composites," *International Materials Reviews*, vol. 49, no. 1, p. 13, 2004.

- [51] A. K.-T. Lau and D. Hui, "The revolutionary creation of new advanced materials—carbon nanotube composites," *Composites Part B: Engineering*, vol. 33, no. 4, pp. 263–277, Jun. 2002.
- [52] "Lightning strike protection for composite structures." [Online]. Available: <http://www.compositesworld.com/articles/lightning-strike-protection-for-composite-structures>. [Accessed: 12-Jun-2012].
- [53] K. Madwar and H. Tarazi, "Desalination techniques for industrial wastewater reuse," *Desalination*, vol. 152, no. 1–3, pp. 325–332, Feb. 2003.
- [54] "Nanomaterials and water purification: Opportunities and Challenges." [Online]. Available: [http://www.ph.ucla.edu/ehs/ehs280/articles/Savage Diallo Review Nanotechnology Water Quality \(Hoek 2\).pdf](http://www.ph.ucla.edu/ehs/ehs280/articles/Savage%20Diallo%20Review%20Nanotechnology%20Water%20Quality%20(Hoek%202).pdf). [Accessed: 11-Jun-2012].
- [55] C. de las Casas and W. Li, "A review of application of carbon nanotubes for lithium ion battery anode material," *Journal of Power Sources*, vol. 208, pp. 74–85, Jun. 2012.
- [56] "New nanostructure for batteries keeps going and going." [Online]. Available: <http://phys.org/news/2012-05-nanostructure-batteries.html>. [Accessed: 11-May-2012].
- [57] Z. Yang, D. Choi, S. Kerisit, K. M. Rosso, D. Wang, J. Zhang, G. Graff, and J. Liu, "Nanostructures and lithium electrochemical reactivity of lithium titanites and titanium oxides: A review," *Journal of Power Sources*, vol. 192, no. 2, pp. 588–598, Jul. 2009.
- [58] J. W. Fergus, "Recent developments in cathode materials for lithium ion batteries," *Journal of Power Sources*, vol. 195, no. 4, pp. 939–954, Feb. 2010.
- [59] K. Jurewicz, E. Frackowiak, and F. Béguin, "Nanoporous H-sorbed carbon as anode of secondary cell," *Journal of Power Sources*, vol. 188, no. 2, pp. 617–620, Mar. 2009.
- [60] W. Choi, S. Hong, J. T. Abrahamson, J.-H. Han, C. Song, N. Nair, S. Baik, and M. S. Strano, "Chemically driven carbon-nanotube-guided thermopower waves.," *Nature materials*, vol. 9, no. 5, pp. 423–9, May 2010.
- [61] N. Li, Y. Huang, F. Du, X. He, X. Lin, H. Gao, Y. Ma, F. Li, Y. Chen, and P. C. Eklund, "Electromagnetic interference (EMI) shielding of single-walled carbon nanotube epoxy composites.," *Nano letters*, vol. 6, no. 6, pp. 1141–5, Jun. 2006.